Volcanic Eruption Forecasting Using Shannon Entropy: Multiple Cases of Study

Pablo Rey-Devesa[1,2], Carmen Benítez[3], Janire Prudencio[1,2], Ligdamis Gutiérrez[1,2], Guillermo Cortés-Moreno[1,2], Manuel Titos[3], Ivan Koulakov[4,5], Luciano Zuccarello[6], and Jesús M. Ibáñez[1,2,7]

[1]Department of Theoretical Physics and Cosmos. Science Faculty. Avd. Fuentenueva s/n. University of Granada. 18071. Granada. Spain.

[2]Andalusian Institute of Geophysics. Campus de Cartuja. University of Granada. C/Profesor Clavera 12. 18071. Granada. Spain.

[3]Department of Signal Theory, Telematics and Communication. University of Granada. Informatics and Telecommunication School. 18071. Granada. Spain.

[4]Trofimuk Institute of Petroleum Geology and Geophysics SB RAS, Prospekt Koptyuga, 3, 630090 Novosibirsk, Russia

[5]Institute of the Earth's Crust SB RAS, Lermontova 128, Irkutsk, Russia

[6]Istituto Nazionale di Geofisica e Vulcanologia, Sezione di Pisa, via Cesare Battisti, 53, 56125, Pisa, Italy.

[7]Istituto Nazionale di Geofisica e Vulcanologia, Sezione di Catania, Piazza Roma, Osservatorio Etneo, Catania, Italy.

Corresponding author: Jesús M. Ibáñez (jibanez@ugr.es)

Key Points:

- While successful volcanic predictions have been achieved, there is no generally valid model suitable for large range of eruptive scenarios.
- We used signal processing techniques to analyze seismic data from five well studied volcanoes to identify short-term eruptive precursors.
- Shannon entropy has a uniform temporal pattern of pre-eruptive change and is a recurrent, transferable and differentiable feature for short-term eruption forecasting.

Abstract

The search for pre-eruptive observables that can be used for short-term volcanic early warning remains a scientific challenge. Pre-eruptive patterns in seismic data are usually identified by analyzing seismic catalogues (e.g., the number and types of recorded seismic events), the evolution of seismic energy, or changes in the tensional state of the volcanic medium as a consequence of changes in the volume of the volcano. However, although successful volcanic predictions have been achieved, there is still no generally valid model suitable for a large range of eruptive scenarios. In this study, we evaluate the potential successful use of Shannon entropy as short-term volcanic eruption forecasting extracted from seismic signals at five well studied volcanoes (Etna, Mount St. Helens, Kilauea, Augustine, and Bezymianny). We identified temporal patterns that can be used as short-term eruptive precursors. We quantified how the Shannon entropy drops several hours before the eruptions analyzed, between 4 days and 12 h before. When Shannon entropy is combined with the temporal evolution of other features (i.e., energy, kurtosis, and the frequency index) and complementary information on types of seismic sources, the meaning of physical changes in the volcanic system could be obtained. Our results show that pre-eruptive variation in Shannon entropy offers is a confident short-term volcanic eruption forecasting tool.

Plain Language Summary

Volcanic eruptions represent a major natural hazard. Despite decades of research, the prediction of volcanic eruptions remains a scientific challenge. Subsurface volcanic processes generate seismic waves, which can be measured at the surface using seismometers. To date, the most successful examples of eruption prediction have been based on seismic data. However, we still lack a prediction model that can be applied across the wide range of eruption styles seen around the world. In this study, we implemented a new approach for the analysis of seismo-volcanic data aimed at forecasting eruptions. We used advanced signal processing algorithms to analyze continuous seismic signals from a suite of well-studied volcanoes (Mount St. Helens, Mt. Etna, Kilauea, Augustine, and Bezymianny) in order to create a new and innovative database of features found within the seismic signals. We found that pre-eruptive variation in the Shannon entropy (a statistical parameter associated to the coherence of the seismic sources) of seismic signals offers a successfully feature for short-term volcanic eruption forecasting. The relationship between pre-eruptive seismic signals and Shannon entropy is based on changes in the probability distributions of the type of seismic waves, independent of the signal source. If this information is combined with other seismic features (e.g., energy, kurtosis, and the frequency index), the actual physical changes in the volcanic system can be identified.

1 Introduction

Volcanic eruptions impact significantly on the Earth and, in particular, on humanity. Although more than 20% of the world population lives under the direct threat of the consequences of volcanic eruptions, currently the advances of the scientific community allow efficient early warning protocols that can save thousands of lives. These advances are based on efficiently interpreting how before an eruption, interactions within the medium cause measurable physical and chemical changes (e.g., Sparks et al., 2012; Girona et al., 2021; Power et al., 2020; Pyle, 2015). Forecasting volcanic eruptions relies on the ability to identify such changes based on the analysis of geophysical and geochemical time series, and in the successful implementation of such data analysis frameworks for pattern recognition in real- or quasi-real-time (e.g., Manga et al., 2017; Dempsey et al., 2020; Girona et al., 2019; Kilburn, 2018; Ardid et al., 2022; Caudron et al., 2020; McKee et al., 2021 a,b). After decades of research, the scientific community is currently having certain degree of success in providing volcanic early warnings to the relevant authorities. However, due to the variety of eruptive styles and the fact that not every unrest episode ends in eruption, forecasting volcanic eruptions remains a challenge (e.g., Jolly et al., 2020; Manley et al., 2021).

Today, society is increasingly demanding efficient short-term early warning protocols (e.g., Thelen et al., 2022) that are sufficiently long to allow for evacuations and/or other defense protocols, but short enough to not lose effectiveness and credibility (Whitehead & Bebbington, 2021). However, identifying short-term volcanic precursors based on broadly-accepted parameters and criteria is a challenging, and as-yet unresolved task. Volcano seismology is one of the most important tools for volcano monitoring and short-term forecasting (McNutt & Roman, 2015; Saccorotti & Lockmet, 2021). Volcanic activity generates a variety of seismic signals that reflect multiple complex processes acting within the volcanic system (e.g., Chouet & Matoza, 2013; Ibáñez et al., 2000), including ground deformations, opening of fractures and conduits, fluids transport and finally a possible eruption. As such, seismic signals contain crucial information for deciphering processes that control the occurrence, timing, and magnitude of eruptions.

Because each process energetically interacts with the environment, generating different energy transients, the result is the presence of a series of seismic-volcanic signals that can be associated with a type of source and a potential evolution of the volcanic system, and even with the possible eruption that we wish to forecast. For this reason, majority forecast models are based on the use of seismic data and the search of the relationship between seismo-volcanic signals, the assessment of their source mechanisms, and volcanic activity models. In this sense, the Generic Swarm Model (McNutt & Roman, 2015) is one of the broadly adopted models to forecasting eruptions using seismic data. However, this is a conceptual

model based on a limited observational database and in where stochastic processes and nonlinear or quasi-stable volcanic behaviors are not considered. In this model the main assumption is volcanic eruptions are preceded by swarms of earthquakes, long period or hybrid event sequences, and tremor. But this model helps forecast volcanic eruptions, and that is why research efforts in recent years have focused on improving our ability to efficiently process large volumes of seismic data. The use of Machine Learning (ML) to study seismo-volcanic signals offers a unique opportunity to obtain maximum information in the shortest time (e.g., Carniel & Guzman, 2021; Malfante et al., 2018 a,b; Manley et al., 2020; Ren et al., 2020). However, the use of ML suffers from a number of limitations when applied to the study of seismic signals: it requires large training datasets of labelled data (e.g., Benítez et al., 2006; Cortés et al., 2019; Di Luccio et al., 2021; Gutiérrez et al., 2009; Ibáñez et al., 2009); several processes can occur simultaneously at the same location, producing a suite of overlapping signals (e.g., Martínez et al., 2021; Titos et al., 2019, 2018a); the non-uniform application of labelling criteria frequently causes confusion when different volcanic scenarios are compared (e.g., Titos et al., 2018b); new advances need to be confirmed using data from dense, permanent, and high-quality seismic networks (e.g., Arámbula-Mendoza et al., 2011; Bueno et al., 2021a; Power et al., 2020; Spampinato et al., 2019).

Contemporaneously, other widely used forecasting models are fundamentally based on the assumption that an acceleration of energy represents an eruption forecast (e.g., Boué et al., 2015, 2016; Power et al., 2013). This idea permitted to include variations of these aspects, such as implementing seismic ratios based on analyzing the energy measured in different frequency bands (Bueno et al., 2019; Caudron et al., 2021; Ardid et al., 2022). Despite their widespread adoption during volcanic crises, significant shortcomings lie in the fact that these models are based on the evaluation of very few parameters (e.g., signal type, number of events). Regardless of these limitations, a number of recent studies have used ML techniques for multi-parametric interpretation of changes in the eruptive states of volcanoes in order to find predictive patterns (e.g., Manley et al., 2021). Bueno et al. (2019) applied Bayesian Neural Network (BNN) methods to frequency analysis of seismic signals at three different volcanoes: Bezymianny, Mount St. Helens, and Mt. Etna and found that the evolution of the uncertainty offers effective eruption short-term early warning that is exportable between volcanic systems. Furthermore, these authors highlighted the importance of analyzing the temporal evolution of seismic features instead of focusing only on the classification of isolated seismic events. Until now, the study of seismic feature evolution has mainly focused on seismic energy (i.e., the real-time seismic amplitude measurement, RSAM; (e.g., Chardot et al., 2015; Endo & Murray, 1991; Ardid et al., 2022) or calculating the energy of earthquakes using their magnitude, their stress release, or the Material Failure Forecasting Method (e.g., Boué et al., 2015, 2016; Cornelius & Voight, 1995; Massa et al., 2016). Satisfactory results have been obtained when applied together with ML methods to obtain the completeness of seismic

149 catalogues (e.g., Alparone et al., 2015; Cortés et al., 2009; Trujillo-Castrillón et al., 2018); however, the
150 resulting models are not exportable to other volcanic systems.

151 In this study, we implemented a new approach for the analysis of seismo-volcanic data aimed at
152 forecasting volcanic eruptions. The previous experience of the study of the seismic features, analyzed on
153 the continuous seismic signal, instead of working with isolated events, allows us to explore new features
154 that could be used as an efficient tool to carry out short term volcanic forecasting. The optimal
155 parametrization of a seismic signal is a crucial issue in seismic signal processing and data analysis.
156 (Alvarez et al. 2011; Cortés et al., 2015; Malfante et al., 2018 a,b). Various methods have been used to
157 transition from the original frame of reference (raw seismograms) to a feature frame. Authors extract
158 parameters (features) from the data and use them to perform a classification of isolated seismic events
159 (e.g., Bueno et al., 2018; Cortés et al., 2014; Titos et al., 2022). These features are mainly grouped into
160 three types according to the information they represent: a) phenomenological features describe
161 seismogram characteristics that are independent of the volcanic system; b) statistical features represent
162 statistical parameters of the waveform and its frequency content; c) signal domain transforms that are
163 determined by applying a transform to the waveform to characterize the signal in a different domain (e.g.,
164 in the frequency domain).

165 Based on these results, we evaluated the potential the pre-eruptive temporal evolution of Shannon
166 entropy for short-term volcanic eruption forecasting. Shannon entropy is a statistical parameter that
167 reveals how similar the seismic signal is to itself in the frequency domain over time. Our starting
168 hypothesis, based on the study of the evolution of energy, is that prior to an eruptive process, all the
169 energy of the volcanic system is addressed to drive the eruption; therefore, the seismic signal should
170 resemble itself, and each time more before the imminent eruption. We used signal processing techniques
171 to analyze continuous seismic signals from five well-studied volcanoes (Mount St. Helens, Mt. Etna,
172 Kilauea, Augustine, and Bezymianny) in order to study the evolution over time of the Shannon entropy to
173 identify potential targets for short-term volcanic eruption forecasting.

174 We believe that our study offer an interesting concept for short-term volcanic forecasting based
175 exclusively on seismology because it is: (a) self-sustaining (it has the ability to carry out volcanic
176 forecasting); (b) agnostic (it does not need established a priori physical models); (c) simple (it is
177 successful with only one input, the seismic signal); (d) direct (it does not need specific previous training);
178 (e) exportable (it can be generalized for different eruptive scenarios); and (f) flexible (it can be adapted to
179 the development of new knowledge). The method presented here can be exported to other volcanoes
180 around the world, offering the potential for high societal impact and widespread interest among the
181 scientific community.

2. Feature extraction and model development

When characterizing the seismic signal, and especially to apply ML studies on isolated seismic events, several authors have highlighted the possibility of using a large number of seismic features, even more than hundreds of them (e.g. Malfante et al., 2018a, b). Cortes et al., 2015, show that this large number of features can be reduced including a set of representative phenomenological, and statistical features in the time and frequency domains. Then, we could transform the original long-term series of seismograms into a multiparametric matrix with the selected extracted features in the time and frequency domain. Among all of them (see supplementary material) we choose the Shannon Entropy to be tested as short-term forecasting feature.

We studied the temporal evolution of the Shannon Entropy to determine if it is evolving in a significant way comparing non-eruptive periods with pre-eruptive and eruptive episodes. It was calculated using the equation from below (Esmaili et al., 2004).

$$-\sum_i P(S_i) log_2 \left(P(S_i)\right) \quad (1)$$

From a statistical perspective, the Shannon entropy of seismic signals has been defined as the distribution of amplitude levels of a given signal (van Ruitenbeek et al., 2020) or a measure of uncertainty in probability distributions (Malfante et al., 2018a). van Ruitenbeek et al. (2020) suggested that amplitude levels of a periodic signal are equally likely and the entropy is high, while a single impulse within a continuous (constant amplitude) signal will have lower entropy. Malfante et al. (2018a) suggested that the maximum Shannon entropy (i.e., the maximum uncertainty) occurs where all possible outcomes have equal probabilities (i.e., a distribution characterized by maximum heterogeneity or randomness), while minimum uncertainty occurs when one possible outcome has a probability of one (i.e., there is no uncertainty and entropy is zero).

In our seismic signals, Shannon entropy represents the uncertainty of the state of the volcanic system and is related to the type of seismic signal. When the seismic signal is composed of random signals originating from different sources (i.e., very broad spectral content), Shannon entropy is high, reflecting the high uncertainty in the types and sources of waves. As such, Shannon entropy provides a quantitative estimate of the homogeneity of the volcanic process. The rapid decrease towards zero reflects a single dominant process within the time and frequency domain that generates seismic waves before an eruption. The seismic source during the eruptive process can manifest in different ways. For example, multiple fractures induce VT earthquakes, bubbles or fluid resonance generate LP-type events, and a

source sustained over time causes volcanic tremor. Each of these source processes results in different energy behaviors (the occurrence of many low energetic events might not show an increase in the energy). However, the evolution of Shannon entropy is always in the same direction; it will decrease towards zero as the state of the volcano evolves towards an eruptive and energetic process.

The detailed workflow developed in this study is shown in Figure 1. This procedure is conceived to extract a single parametric analysis (obtaining a vector) or a multi-parametric feature study (obtaining a matrix of features). We only used the vertical component of the seismic signal because at the present many volcanoes continue being seismically controlled by one component seismometer, and one of the scopes of this work is to generalize the results. The first step is to filter the signal using a bandpass filter from 1 to 16 Hz to reduce sources of noise. Below 1 Hz, the influence of the oceanic load over the seismic signal is too strong and must be removed according to the results of Almendros et al. (2007); at frequencies of > 15–20 Hz, climatic and anthropic conditions (wind, rain, traffic, etc.) affect the seismic signals. For each seismogram, selected an interval of time (1 or 10 min overlapped by 50%, according the volcano) over which the parametric transformation is computed.

As indicated above, we should expect that previous to an eruptive episode the Shannon Entropy must evolve towards zero, or reaching a minimum. In order to quantify the decay of this feature we used a widely accepted algorithm like STA/LTA. We estimated the mean value of the Shannon entropy for each volcano during resting periods (SE_0) and implemented small windows of analysis to calculate how the Shannon entropy was evolving (SE(i)) according to this resting value, using the formula from below. In average the LTA value was estimated in an interval of 20 days of volcanic repose for each volcano. The STA has the same duration of the window used to feature extraction analysis (from 1 to 10 minutes). We then established a threshold which allows us to forecast the eruption without having false alerts (equation 2). When the value of the decay remains over the 70%, i.e. the STA is lower than 30% of the LTA value, we consider this is the starting of the potential short term forecast interval. The value of 70% of threshold is an experimental and compromise value based on the generic value used in many research works to determine the error interval of experimental results. It is clear that increasing this value of threshold the short-term forecasting period would be reduced, but reducing it we have the chance to have several false alarms.

$$Decay\ Ratio\ [\%] = 100 \cdot \left(1 - \frac{SE(i)}{SE_0}\right) \qquad (2)$$

3. Data and volcanic scenarios

We selected data from five well-studied volcanoes (Mt. Etna, Mount St. Helens, Augustine, Bezymianny, and Kilauea); Table 1 represents a broad range of volcanic processes and eruption styles, as long as several eruptive mechanisms, showing different pre-eruptive seismic patterns with different kind of signals (volcano-tectonic, long period, volcanic tremor, etc.). This makes this comparison among them interesting to test the exportability of our hypothesis. For each volcanic scenario, if available, we analyzed several seismic stations but here will we only present results of one station per eruptive scenario, selected based on proximity to the eruptive center and/or the completeness of the seismic catalogue (Figure 2). We want to emphasize that the volcanoes Mt. Etna, Bezymianny and Mount St. Helen have been selected, in addition to their interest based on their eruptive history, because they were the volcanoes studied by Bueno et al., (2021 a,b) where it was observed how uncertainty could be used as a forecasting indicator.

The selection of the databases was conditioned on the availability of public data available online in repositories such as IRIS, or based on data acquired by our work team in temporary field campaigns or through institutional agreements. The corresponding section presents the links to access all the data used for this analysis. The eruptive processes selected for study have been selected based on different reasons: a) relevance of the eruptions, as is the case of Augustine 2006, Mount St. Helens 2004, Kilauea, 2018; b) have been previously analyzed using uncertainty, such as Mt. Etna, 2013, Bezymianny 2007; c) have a long series of quality seismic records and have an eruptive event recorded on video and an eruptive column more than 11 km high, in the case of the Bezymianny 2017 volcano. Noteworthy, even if public repositories offer available volcanic seismic data, long time series of them are not always accessible and only short time intervals around some specific volcanic events are uploaded with enough quality to be successfully analyzed.

The eruption of Mount St. Helens (2004) represents the reawakening of this volcano after more than 10 years of calm (Iverson et al, 2006). Itself the size of this eruption is not too large, but it was forecasted by intense seismicity of volcanic tectonic earthquakes and followed by an energetic volcanic tremor prior the explosion of the extruded dome. The eruption of Augustine volcano was a moderate explosion (VEI 3) with an unrest characterized by intense seismicity lasting at least 5 months prior the eruption of 11 of January, 2006 (Manley et al. (2021). This eruption is characterized by two explosions within 30 minutes detected by satellite observations Bailey et al., (2006), generating ash plumes to maximum heights of 6.5 and 10.2 km respectively. This eruptive phase lasted 17 days with at least 14 representative explosions. The Kilauea volcano eruption of 2018 represents a special case within the eruptive mechanism of this volcanic system. The eruption is preceded by a collapse of part of the building that occurs on the night of April 30. Several days later, on May 3, the first fissures appear with the

278 emission of lava flows. Finally, on May 5, an earthquake of magnitude Mw 6.9 occurred on the flank of
279 the building, which ended up opening more fissures and larger lava flows (Patrick et al., 2020). Since
280 approximately the year 2000, the Mt Etna volcano has had a continuous eruptive activity, alternating lava
281 flows, lava fountains and some moderate explosive episodes (Spampinato et al., 2019). In general,
282 seismic activity is represented by the occurrence of shallow volcano tectonic earthquakes, long period
283 events and continuous volcanic tremor (Zuccarello et al., 2022). For this analysis we have selected four
284 episodes of lava fountains from 2013, previously studied by Bueno et al. (2021 a,b) and which were
285 forecasted by a strong volcanic tremor and absence of VT earthquakes. For Bezymianny volcano we
286 selected two eruptive phases. In the first one, in 2007, it was observed how the uncertainty always
287 decreased prior to each of the three selected explosions, being the initial motivation of this work. In 2017
288 the Institute of Volcanology and Seismology of the Russian Academic of Sciences (Koulakov et al, 2021)
289 organized a temporary seismic experiment deploying several Broad Band stations around the volcano. On
290 December 20, 2017 a large volcanic explosion occurred with an eruptive column at least 11 km high that
291 will be analyzed in detail later. The advantage of this experiment is that we have a full year of data
292 available, continuously, at various stations. This will allow us to study in depth if the Shannon Entropy
293 can be considered as a recurrent and differentiable parameter as an element of short-term volcanic
294 forecasting as Ardid et al., (2022) define to be used in a general way in early warning volcanic eruption
295 protocols.

296 **4. Results.**

297 The first step to ensure that the idea that the Shannon Entropy is used as a reliable parameter as a
298 forecast of volcanic eruption is to check if it meets the requirements indicated by Ardid et al., (2022).
299 These authors define an eruption precursor as a common pattern that has to be recurrent (occurs prior to
300 multiple events), transferable (occurs prior to eruptions at different volcanoes) and differentiable (absent
301 during non-eruptive unrest and volcanic repose). In advance, we explain why we consider Shannon
302 entropy a differentiable parameter.

303 For this, it is necessary to study long time series. It is evident that the longer the time series, even
304 years, the better, but the continuous availability of data, without interruptions and with the same recording
305 system is a complex task. On the base of the advantage of the seismic experiment performed in
306 Bezymianny volcano we have the capability to analyze a whole year of high-quality data from continuous
307 seismic signals. In this period, we can identify both resting periods and pre-eruptive activity before the
308 energetic explosion of December 20, 2017. We considered these data reliable enough to trust the results
309 obtained and proceed to test the method in different eruptive episodes of this volcano, and also in
310 different volcanoes.

311 Systematic analysis of Shannon entropy at Bezymianny from August 2017 to July 2018 (Figure
312 3) revealed that generally, the mean values obtained remain high. However, we observed some intervals
313 in which this trend decays to lower values. As described above we defined a significant decrease of the
314 values of the Shannon Entropy when the STA value decays until more than the 70% of the LTA value.
315 Following this rule, we detected few intervals with this pattern. The biggest decay occurred in the instant
316 of the largest volcanic explosion of December, 20th 2017 (the STA value 98.3% lower than the LTA one).
317 In addition, low Shannon entropy values were observed on other intervals with decays lower than 70 %.
318 Analyzing data from the KBGS (Kamchatka Branch Geophysical Survey) institution two important
319 explosions were reported at the neighboring Kliuchevskoy volcano (August 2017 and May 2018). Both
320 eruptions are clearly aligned with the first and last drops in Shannon entropy (marked as a red shadow
321 area in figure 3). We suggest that these low Shannon entropy anomalies are potential forecasting
322 evidences of the explosions at Kliuchevskoy volcano. The relatively lower value reached for the
323 Bezymianny event likely reflects the closer distance to the seismic station (BZ01 is < 2 km from the
324 summit of Bezymianny and ~10 km from the summit of Kliuchevskoy; Figure 2). The recorded
325 Kliuchevskoy signals at BZ01 station likely suffered seismic attenuation effects and interference by local
326 signals and other sources of noise. There is a minimum of short duration located on September 2017
327 associated with a local earthquake of magnitude Mw 4.3 as reported in IRIS institution. The decrease
328 observed in March 2018 is associated to an intense volcanic tremor recorded in the volcanic area triggered
329 by another local earthquake of Mw 4.5 (reported in IRIS). We have no evidences of potential volcanic
330 eruptions or lava dome growth that could be associated with this activity, but the presence of this intense
331 volcanic tremor confirms its volcanic source. Finally, during April 2018 an intense volcano-tectonic
332 earthquake swarm was recorded, associated with a set of three minimum values of the Shannon Entropy.
333 According to these observations, and at least for the period of time analyzed, the significant decreases in
334 the Shannon Entropy values seem to be exclusively associated with eruptive processes.

335 The next step is determining if this decrease in Shannon entropy values can be quantified as a
336 promising evidence of short-term volcanic forecasting tool. In figure 4 we show the evolution of the
337 Shannon Entropy a week prior to the explosion of December 20, 2017. The STA/LTA ratio was computed
338 and in shadow green we highlight the instant in which the decay is continuously lower than the 70% (the
339 vertical red line marks the instant of the eruptive process). Notice that its continuous decay appears two
340 days before the eruption, reaching values close to zero in the moment of the explosion (as indicated above
341 a decay of 98.3%). However, as marked in figure 4, at least 5 days before we can consider potential
342 forecasting evidences.

Referring to the three explosions of the Bezymianny volcano in 2007, this same procedure for estimating the decay of the STA/LTA ratio of the Shannon Entropy was repeated. In figure 5 we plot these results. As observed in all cases there were a minimum value of the Shannon Entropy at the instant of the volcanic explosion (marked with a red line). These decays were of 99.5%, 99.5% and 100% respectively. Notice as the pre-eruptive forecasting interval change according each explosion, from 1 hour to a day. According the analysis of Bueno et al. (2021 a,b) it seems to be an inverse relationship pre-eruptive forecasting interval duration and energy of the explosion, since the larger explosion occurred on October 14, 2007 and it has the largest pre-eruptive evidences.

The analysis of the 4 lava fountain episodes recorded at Mt. Etna in November 2013 is plotted in Figure 6. As noticed in the precedent analysis we observed a significant decrease (below the marked threshold) prior every paroxysm. In all cases, as in Bezymianny, just when the Shannon Entropy start to decrease below the threshold, this is a stable decreasing tendency marking without doubts that some volcanic energetic process will happen, reaching its minimum at the moment of every eruptive episode (in this case lava fountains, marked in red), 98.4%, 98.9%, 97.4% and 95.1% respectively. The short-term pre-eruptive intervals were 12h, 18h, 3 h and 2 h respectively and according again with the size of each volcanic episode.

Finally, we applied the procedure to the rest of the volcanic scenarios (Mount St. Helens, Augustine and Kilauea), plotted in Figure 7. In the case of Mount St. Helens and Augustine the decay of the Shannon Entropy is 100% and 96.8% respectively. Noteworthy, as indicated above, the analyzed Augustine eruption is characterized by two moderate/large explosions (marked in Figure 7 with two red lines). The proposed approach identifies well the instant of the first explosion with the highest decay of the Shannon Entropy value. Their respective short-term forecasting intervals were 4 days and 12 hours. The case of Kilauea is much more complex, observing different decays according the three different processes described above. The decay of the Shannon Entropy reaches 99.1% when the summit collapsed, 80.7% when the first fissure and lava flow appeared, and 98.0% when the 6.9 Mw earthquake occurred. There is no measurable forecasting interval for the collapse of the summit and the potential failure of this decay will be discussed in next section.

Thus, we propose, according to Ardid et al., (2022), Shannon entropy is a short-term eruptive precursor, and demonstrated to be recurrent (occurs prior to every eruption studied), transferable (occurs in different volcanoes with different pre-eruptive behavior) and differentiable, as it only changes whenever an eruption occurs, as we conclude after analyzing a year of data recorded continuously.

5. Discussion.

After studying 5 different volcanoes with different eruptive sources, lava types and pre-eruptive behavior we demonstrated the Shannon entropy approach works efficiently as short-term volcanic eruption forecasting tool independently of the eruptive mechanism. In addition, it is interesting to notice each volcanic process is dominated for different pre-eruptive type of seismic signals. We have examples of eruptions driven by volcano-tectonic events, like Bezymianny 2017 (Koulakov et al., 2021); others by mainly volcanic tremor like Mt. Etna (Spampinato et al., 2019) or another like Mount St. Helens with the presence of mixed seismicity, first intense swarm of volcano-tectonic events and later by volcanic tremor (Lehto et al., 2010). In order to quantify objectively the evolution of the Shannon Entropy and therefore to use it as an accurate short-term forecast volcanic eruptions tool we used an STA/LTA algorithm quantifying the decay ratio. This procedure permits to objectively identify the time intervals in which we can consider we are a pre-eruptive period. As we indicated above the developed approach has some important advantages as a powerful tool: it is agnostic (it does not need established a priori physical models); it is simple (it is successful with only one input, the seismic signal); it is direct (it does not need specific previous training). That is, we can obtain a pre-eruptive indicator without knowing what is the physical mechanism that dominates the eruption, without having previously trained the system for each different eruptive scenario and of easy integration in the procedures of surveillance in real time.

It is interesting to combine our results with another pre-eruptive seismic evidences to better understand their physical meaning. As Kilburn (2018) indicated ground deformation, volcanic seismicity (mainly VT events) and their associated energy release could be considered one of the most reliable pre-eruptive evidences. As is broadly known, scientific community has been using the energy of the seismic signal to forecast volcanic eruptions (Ortiz et al. 2003; Boue et al., 2016; Power et al., 2013) and recently some variations of the use of the energy have obtained promising results (Caudron et al., 2021; Dempsey et al., 2020; 2022). Despite of several successfully results, some limitations were found. For example, the energy reflects the size of the seismicity prior to an eruption; more energetic events will display bigger energy values independently if they are directly linked with the eruptive process. In addition, the energy is a growing parameter and to determine its maximum or its exactly timing relationship when the eruption will happen is a complex task.

In some volcanoes it is possible to access to seismic catalogs and perform additional analysis on the registered seismicity. We have evidences that some seismic features (see supplementary material) are directly related to the type of seismicity, and therefore to the earthquake-volcanic source. These features can reflect changes in the seismic signal patterns, and they could be associated with possible physical models. Thus, to analyze these patters we transform the original features vector into a features matrix, as

highlighted in Figure 1. As Cortés et al. (2015) and Bueno et al., (2021 a,b) indicated, the Kurtosis and the Frequency Index can be used as indicators of the type of recorded seismic events and their evolution according changes in the volcanic system. The Kurtosis (eq. 3) evaluates how the frequencies of the signal are distributed, and the Frequency Index (eq. 4) takes into consideration the ratio of the energy content between high and low frequencies of the signal (we considered low frequencies between 1-6 Hz, and high frequencies between 6-16 Hz). Therefore, their changes can be directly associated to changes or evolution in the seismic sources.

$$KUR = \frac{1}{n}\sum_i \left(\frac{S[i]-\mu_s}{\sigma_s}\right)^4 \quad (3)$$

$$FI = log_{10}\left(\frac{E_{high\ frequencies}}{E_{low\ frequencies}}\right) \quad (4)$$

VT events recorded in a near field have high frequency contains in confront to the background signal, making increase the obtained value of the Kurtosis, as observed by Bueno et al., (2021a). In addition, a shift of the seismic foci from depth to the surface will include an enrichment of the high frequency contains of the signals (since the seismic attenuation will be less effective) showing again increases in the value of the Kurtosis. On the other hand, volcanic tremor is dominated by lower frequency signals (Konstantinou and Schlindwein, 2003; Zuccarello et al., 2022). Therefore, the increasing of the volcanic tremor should move the Frequency Index toward negative values in comparison to the background signal. In other word, the kurtosis is more sensitive to the occurrence of VTs and the Frequency Index to the occurrence of volcanic tremor.

To show the relationship between Kurtosis and occurrence of VTs we will study the case of the Bezymianny eruption of December 20th, 2017. Koulakov et al, (2021) indicated the occurrence of an intense seismic swarm prior the eruption, however there is no a complete seismic catalogue of this period. Using Hidden Markov Model (HMM) we were able to obtain a VT seismic catalogue of Bezymianny for the whole month of December 2017 (Benítez et al., 2006; Ibáñez et al., 2009; Cortés et al., 2021). Simultaneously we computed the Kurtosis using the same window length as for the Shannon Entropy. In Figure 8 we compare the variations of the Kurtosis and the cumulative number of VTs for intervals 1 h long. As observed, both evolve in parallel in the days before the eruption. The green shadow area represents the pre-eruptive short-term forecasting interval predicted by the Shannon Entropy with the 70% of decay threshold. Notice as these three parameters seem to evolve in a similar way. The advantage to use the seismic features in confront to the identification of seismic events is the faster evaluation procedure and the absence of previous training process (the application of the HMM to obtain a realizable seismic catalog takes longer time). On the other hand, a seismic catalogue itself is not a direct eruptive

precursor, since it is the input of different precursory algorithms that evaluate the probability of an eruption. However, the evolution of the seismic features could be used directly as precursors.

However, not all eruptions have VT swarms as precursory activity, as it was the case of the lava fountains of Mt. Etna occurred in 2013. The Frequency Index reflects the temporal variation of the spectral relationship between certain frequency bands, even if it has a complex interpretation. These changes may reflect different volcanic dynamics, both in terms of source and medium; for example, the appearance of VTs, LPs, or tremor could be linked with an increase in the frequency index, and sometimes with a decrease. As the volcano deforms (inflates) prior to an eruption, the increase in system stress will shift the spectral content of the signal towards high frequencies; deflation would shift the spectral content of the signal towards low frequencies. A change in the impedance contrast at the source, or in the volcanic system, would also cause changes in spectral content. Impedance is the ratio between the elastic properties of confining (volcanic fluids) and confined, the volcanic edifice (Chouet & Matoza, 2013). Thus, evolution of a resonant system from a "dry" or pure gas to ash-rich content would lead to a shift towards low frequencies, and vice versa. The geometry of the system affects the frequency index, as does magma ascent, which is associated lower frequencies of tremor. In summary, changes in the frequency index are a common pre-eruptive observation, but the style of variation depends on many factors that cannot be controlled a priori, precluding its use in early warning. However, there are “easier” situations as was the case of Mt. Etna in 2013. The volcanic tremor of Mt. Etna uses to appear at frequencies between 1 to 3 Hz (Zuccarello et al., 2022) and the background seismic signal is over 6 Hz (seismic noise). Therefore, it is expected that the Frequency Index must be shifted towards negative values as the volcanic tremor is increasing. In parallel the energy of the seismic signal should increase too. To confirm this hypothesis, we evaluated the temporal evolution of the Frequency Index and the Energy for the Mt. Etna lava fountains and compared them with the evolution of the Shannon Entropy (Figure 9).

Notice as when the volcanic tremor appeared we observed a sudden change in both, Shannon Entropy (moving toward zero), the Frequency Index (moving toward negative values) and Energy (growing significantly). All used parameters marked a clear pre-event time. However, the Shannon Entropy is the only one feature which trend could be associated with the timing of the eruption (marked in the moment of the lower value, 98.4% lower than the LTA). The energy continues growing until the paroxysmal moment of high energetic lava fountain; meanwhile the Frequency Index reveals the different mechanism associated to the eruption and timing of the tremor appearance, with a non-homogeneous pattern.

The two previous examples were dominated by a single type of seismicity, VT events for Bezymianny and volcanic tremor of Mt. Etna. The Mount St. Helens eruption of 2004 is an example of multiple pre-event seismicity, as indicated above. In Figure 10 we plot the temporal evolution of the three features introduced in this section. Green region represents the moment when the Shannon entropy decays over the 70%. The energy starts its growth more than a day and a half later than the instant the Shannon entropy works as short-term forecast indicator. In addition, the energy reaches a maximum and then decrease, without erupting yet. Notice the high values of the cumulative Kurtosis between the days 25 and 28 reflects the high number of VT events detected. Later, the pre-eruptive process starts to be dominated by the volcanic tremor, as reflected by the negative values of the Frequency Index and the decrease of the Kurtosis.

It is noteworthy that kurtosis and the frequency index cannot be used individually as universal predictive elements. However, when combined with the Shannon Entropy, they provide information on the type of prevailing seismic activity, the medium, elastic properties, and more; they are therefore useful for investigating the mechanisms of the volcanic source.

Previous studies have shown that Entropy can be used to characterize very energetic seismic series or catastrophic energetic events (e.g., Posadas et al., 2021). To identify potential external factors that could affect entropy, we selected a fifth volcanic scenario with completely characteristics—the April–May 2018 eruption of Kilauea. This eruption was preceded by a caldera collapse and subsequent Mw 6.9 earthquake. A proposed triggering mechanism was precipitation (Farquharson & Amelung, 2020), which may have changed the pore pressure in the rift zone. Figure 7c shows Shannon entropy and seismic energy from April 29 to May 7, 2018. Sharp drops, with the values approaching zero, occurred at the same time as (but not before) the caldera collapse and earthquake. Then, during the eruptive episode, Shannon entropy remained very low. As such, Shannon entropy was not a precursory feature.

If rainfall was the eruption trigger, the eruption was not a classic example of an inner-source driven volcanic system, but was a sudden eruptive phenomenon triggered by external factors. This could explain why pre-eruptive Shannon entropy was not a suitable precursory indicator for this unrest. Based on this example, we suggest that decreasing Shannon entropy towards zero can only be for short-term early warning in systems controlled by internal factors; those eruptions triggered by external events (e.g., heavy rainfall) cannot be predicted using this method.

As a resume:

a) We observed that in all analyzed volcanic scenarios there is always a quantitatively evaluated decrease of the Shannon Entropy prior to different type of eruptions independently of the characteristics of pre-eruptive state and seismic sequences. Therefore, is a good "agnostic" short-term volcanic eruption forecast indicator.

b) The Shannon Entropy remains high and almost constant when the volcano is resting or when the activity is minor.

c) In all cases the energy is a valuable feature to confirm this observation, but it does not always be used as short-term forecasting feature.

d) The use of other seismic parameter, such as Kurtosis or Frequency Index, helps to constrain potential physical models driving the eruption.

e) We suggest the use of this seismic feature since it is fast and easy to implement, works in real time, it does not need previous training and it is transferable among different volcanoes.

6. Conclusions

The results of this study suggest that the Shannon entropy of pre-eruptive seismic signals offers a robust and reliable feature for short-term volcanic eruption forecasting. Comparing the energy evolution and the Shannon entropy we can find some interesting features. The main observation is Shannon Entropy is inversely proportional to the log energy, entropy decays to zero when the system reorganizes itself and the signals are more similar between them, allowing us to easily identify changes in the volcanic system. The relationship between pre-eruptive seismic signals and Shannon entropy is direct and based on changes in the probability distributions of the type of seismic waves, independent of their source. As a uniform volcanic source processes towards an eruption there is high homogeneity of recorded seismic wave types, regardless of the energy and underlying source processes. This homogeneity can be measured quantitatively through the Shannon entropy and the trend towards zero will mark the imminent start of the volcanic eruption.

Combining this with other features, such as energy, kurtosis, frequency index and interesting parameters selected in future works, offers even greater predictive certainty, along with insight into the types of seismic sources and physical changes in the volcanic system. In general, this approach is exportable from one volcanic system to another. However, it falls short of universality because eruptions triggered by external processes (e.g., rainfall) cannot be predicted in this way. Shannon entropy is simple and rapid to evaluate, and the relevant pre-eruptive changes (i.e., a decrease towards zero) occur over

intervals of between 4 days and 12 h prior to eruption, which is sufficient for the relevant authorities to implement alert and evacuation protocols.

Acknowledgments

This study was partially supported by the Spanish FEMALE (PID2019-106260GB-I00) and PROOF-FOREVER (EUR2022.134044) projects. P. Rey-Devesa was funded by the Ministerio de Ciencia e Innovación del Gobierno de España (MCIN), Agencia Estatal de Investigación (AEI), Fondo Social Europeo (FSE), and Programa Estatal de Promoción del Talento y su Empleabilidad en I+D+I Ayudas para contratos predoctorales para la formación de doctores 2020 (PRE2020-092719). Ivan Koulakov was supported by the Russian Science Foundation (Grant No. 20-17-00075). Luciano Zuccarello was supported by the INGV Pianeta Dinamico 2021 Tema 8 SOME project (grant no. CUP D53J1900017001) funded by the Italian Ministry of University and Research "Fondo finalizzato al rilancio degli investimenti delle amministrazioni centrali dello Stato e allo sviluppo del Paese, legge 145/2018". English language editing was performed by Tornillo Scientific, UK.

Data availability statement

Data of the five volcanoes analyzed in this work are publically accessible in the links that will be detailed below. The used software of this work (all programmed developed by us) are also publically accessible (link provided below) and are also presented with specific use examples to be able to independently reproduce all the results obtained in this work. The repository sites used are stable, publically accessible for free and recognized by the scientific community.

1.- Agustine Volcano (2006) data were obtained by using the facilities of IRIS Data Services, and specifically the IRIS Data Management Center. Direct links to access to the data of this volcano are:

https://ds.iris.edu/mda/AV/

https://ds.iris.edu/mda/HV/JOKA/?starttime=2012-09-17T00:00:00&endtime=2599-12-31T23:59:59

2.- Kilauea Volcano (2018) data were obtained by using the facilities of IRIS Data Services, and specifically the IRIS Data Management Center. Direct links to access to the data of this volcano are:

https://ds.iris.edu/mda/HV/

https://ds.iris.edu/mda/HV/JOKA/?starttime=2012-09-17T00:00:00&endtime=2599-12-31T23:59:59

559 3.- Mount St. Helens (2004) data were obtained by using the facilities of IRIS Data Services, and
560 specifically the IRIS Data Management Center. Direct links to access to the data of this volcano are:

561 https://ds.iris.edu/mda/UW/

562 https://ds.iris.edu/mda/UW/SHW/?starttime=1972-10-01T00:00:00&endtime=2599-12-
563 31T23:59:59

564 4.- Bezymianny volcano.

565 Data from 2007 were obtained by using the facilities of IRIS Data Services, and specifically the
566 IRIS Data Management Center.

567 Data for the temporary experiment (2017-2018) are available in the compressed folder
568 "Dataset_volcanoes.Rar", located in the ZENODO repository at the following address and DOI.

569 https://doi.org/10.5281/zenodo.6821530

570 https://zenodo.org/record/6821530#.YvyeUS7P1PY

571 5.- Etna volcano data (2013) are available in the ZENODO repository at the following address
572 and DOI.

573 https://doi.org/10.5281/zenodo.6849621

574 https://zenodo.org/record/6849621#.YvyetS7P1PY

575 B) Instructions for downloading the data associated with the IRIS network, as well as the access
576 to the download software developed by us, can be found in the "Readme.txt" file, available in the
577 ZENODO repository at the following address and DOI.

578 https://doi.org/10.5281/zenodo.6821530

579 https://zenodo.org/record/6821530#.YvyeUS7P1PY

580 C) The seismic parameter analysis software, with illustrative examples to be able to reproduce
581 our results, are available in the compressed folder "Software.Rar", located in the ZENODO repository at
582 the following address and DOI.

583 https://doi.org/10.5281/zenodo.6821530

584 https://zenodo.org/record/6821530#.YvyeUS7P1PY

585 D) The software related to the automatic recognition of seismic signals used for the study of the
586 Bezymianny volcano is developed under the EU project called VULCAN.ears located in the ZENODO
587 repository at the following address and DOI.

https://zenodo.org/record/3594080#.YvydiC7P1PY

https://zenodo.org/record/4305100#.Yvydti7P1PY

https://doi.org/10.5281/zenodo.4305100

References

Almendros, J., Ibáñez, J. M., Carmona, E., & Zandomeneghi, D. (2007), Array analyses of volcanic earthquakes and tremor recorded at Las Cañadas caldera (Tenerife Island, Spain) during the 2004 seismic activation of Teide volcano. *Journal of Volcanology and Geothermal Research*, *160*(3–4), 285–299. doi:10.1016/j.jvolgeores.2006.10.002

Aloisi, M., Bonaccorso, A., Cannavò, F., Currenti, G., & Gambino, S. (2020), The 24 December 2018 eruptive intrusion at Etna volcano as revealed by multidisciplinary continuous deformation networks (CGPS, Borehole Strainmeters and Tiltmeters). *Journal of Geophysical Research: Solid Earth, 125*(8), doi:10.1029/2019JB019117

Alparone, S., Maiolino, V., Mostaccio, A., Scaltrito, A., Ursino, A., Barberi, G., et al. (2015), Instrumental seismic catalogue of Mt. Etna earthquakes (Sicily, Italy): ten years (2000–2010) of instrumental recordings. *Annals of Geophysics*. doi:10.4401/ag-6591

Alvarez, I., Garcia, L., Cortes, G., Benitez, C., & De la Torre, Á. (2011), Discriminative feature selection for automatic classification of volcano-seismic signals. *IEEE Geoscience and Remote Sensing Letters, 9*(2), 151–155. doi:10.1109/LGRS.2011.2162815

Anderson, K., & Segall, P. (2013), Bayesian inversion of data from effusive volcanic eruptions using physics-based models: Application to Mount St. Helens 2004–2008. *Journal of Geophysical Research: Solid Earth, 118*(5), 2017–2037. doi:10.1002/jgrb.50169

Arámbula-Mendoza, R., Lesage, P., Valdés-González, C., Varley, N. R., Reyes-Dávila, G., & Navarro, C. (2011), Seismic activity that accompanied the effusive and explosive eruptions during the 2004–2005 period at Volcán de Colima, Mexico. *Journal of Volcanology and Geothermal Research, 205*(1–2), 30–46. doi:10.1016/j.jvolgeores.2011.02.009

Ardid, A., Dempsey, D., Caudron, C., & Cronin, S. (2022), Seismic precursors to the Whakaari 2019 phreatic eruption are transferable to other eruptions and volcanoes. *Nature Communications, 13*(1), 1–9. doi:10.1038/s41467-022-29681-y

Bailey, J. E., Dean, K. G., Dehn, J., Webley, P. W., Power, J., Coombs, M., & Freymueller, J. (2006). Integrated satellite observations of the 2006 eruption of Augustine Volcano. The, 481-506.

618 Barreca, G., Branca, S., Corsaro, R. A., Scarfì, L., Cannavò, F., Aloisi, M., et al. (2020), Slab detachment,
619 mantle flow, and crustal collision in eastern Sicily (southern Italy): Implications on Mount Etna
620 volcanism. *Tectonics, 39*(9), doi:10.1029/2020TC006188.

621 Barreca, G., Branca, S., & Monaco, C. (2018), Three-Dimensional Modeling of Mount Etna Volcano:
622 Volume Assessment, Trend of Eruption Rates, and Geodynamic Significance. *Tectonics, 37*(3),
623 842–857. doi:10.1002/2017TC004851

624 Benítez, M. C., Ramírez, J., Segura, J. C., Ibanez, J. M., Almendros, J., García-Yeguas, A., & Cortes, G.
625 (2006), Continuous HMM-based seismic-event classification at Deception Island, Antarctica.
626 *IEEE Transactions on Geoscience and Remote Sensing, 45*(1), 138–146.
627 doi:10.1109/TGRS.2006.882264

628 Berlo, K., Blundy, J., Turner, S., Cashman, K., Hawkesworth, C., & Black, S. (2004), Geochemical
629 precursors to volcanic activity at Mount St. Helens, USA. *Science, 306*(5699), 1167–1169.
630 doi:10.1126/science.1103869

631 Bonaccorso, A., Calvari, S., Linde, A., & Sacks, S. (2014), Eruptive processes leading to the most
632 explosive lava fountain at Etna volcano: The 23 November 2013 episode. *Geophysical Research*
633 *Letters, 41*(14), 4912–4919. doi:10.1002/2014GL060623

634 Boué, A., Lesage, P., Cortés, G., Valette, B., & Reyes-Dávila, G. (2015), Real-time eruption forecasting
635 using the material Failure Forecast Method with a Bayesian approach. *Journal of Geophysical*
636 *Research: Solid Earth, 120*(4), 2143–2161. doi:10.1002/2014JB011637

637 Boué, A., Lesage, P., Cortés, G., Valette, B., Reyes-Dávila, G., Arámbula-Mendoza, R., & Budi-Santoso,
638 A. (2016), Performance of the 'material Failure Forecast Method'in real-time situations: A
639 Bayesian approach applied on effusive and explosive eruptions. *Journal of Volcanology and*
640 *Geothermal Research, 327*, 622–633. doi:10.1016/j.jvolgeores.2016.10.002

641 Bueno, A., Titos, M., García, L., Álvarez, I., Ibañez, J., & Benítez, C. (2018), Classification of volcano-
642 seismic signals with Bayesian neural networks. Proceedings of the 26th IEEE European Signal
643 Processing Conference (EUSIPCO), 2295–2299

644 Bueno, A., Benitez, C., De Angelis, S., Moreno, A. D., & Ibáñez, J. M. (2019), Volcano-seismic transfer
645 learning and uncertainty quantification with Bayesian neural networks. *IEEE Transactions on*
646 *Geoscience and Remote Sensing, 58*(2), 892–902. doi:10.1109/TGRS.2019.2941494

Bueno, A., Titos, M., Benítez, C., & Ibáñez, J. M. (2021a), Continuous Active Learning for Seismo-Volcanic Monitoring. *IEEE Geoscience and Remote Sensing Letters, 19*, 1–5. doi:10.1109/lgrs.2021.3121611

Bueno, A., Benítez, C., Zuccarello, L., De Angelis, S., & Ibáñez, J. M. (2021b), Bayesian monitoring of seismo-volcanic dynamics. IEEE Transactions on Geoscience and Remote Sensing, 60, 1–14. doi:10.1109/TGRS.2021.3076012

Buurman, H., & West, M. E. (2006), Seismic precursors to volcanic explosions during the 2006 eruption of Augustine Volcano. In J. A. Power, M. L. Coombs, and J. T. Freymueller (Eds.), *The 2006 Eruption of Augustine Volcano, Alaska* (pp. 41–57). U.S. Geological Survey Professional Paper 1769. https://pubs.usgs.gov/pp/1769/chapters/p1769_chapter02.pdf

Carniel, R., & Guzmán, R. S. (2021), Machine learning in volcanology: a review. In K. Németh (Ed.), *Updates in Volcanology—Transdisciplinary Nature of Volcano Science*. IntechOpen. doi:10.5772/intechopen.94217

Chardot, L., Jolly, A. D., Kennedy, B. M., Fournier, N., & Sherburn, S. (2015), Using volcanic tremor for eruption forecasting at White Island volcano (Whakaari), New Zealand. *Journal of Volcanology and Geothermal Research, 302*, 11–23. doi:10.1016/j.jvolgeores.2015.06.001

Chouet, B. A., & Matoza, R. S. (2013), A multi-decadal view of seismic methods for detecting precursors of magma movement and eruption. *Journal of Volcanology and Geothermal Research, 252*, 108–175. doi:10.1016/j.jvolgeores.2012.11.013

Coombs, M. L., Bull, K. F., Vallance, J. W., Schneider, D. J., Thoms, E. E., Wessels, R. L., & McGimsey, R. G. (2010), Timing, distribution, and volume of proximal products of the 2006 eruption of Augustine Volcano. In J. A. Power, M. L. Coombs, and J. T. Freymueller (Eds.), *The 2006 Eruption of Augustine Volcano, Alaska* (pp. 145–185). U.S. Geological Survey Professional Paper 1769. https://pubs.usgs.gov/pp/1769/chapters/p1769_chapter08/p1769_ch08_text.pdf

Cornelius, R. R., & Voight, B. (1995), Seismological aspects of the 1989–1990 eruption at Redoubt Volcano, Alaska: The Materials Failure Forecast Method (FFM) with RSAM and SSAM seismic data. *Journal of Volcanology and Geothermal Research, 62*(1–4), 469–498. doi:10.1016/0377-0273(94)00078-U

Cortés, G., Arámbula, R., Gutiérrez, L., Benítez, C., Ibánez, J., Lesage, P., et al. (2009), Evaluating robustness of a HMM-based classification system of volcano-seismic events at colima and

677 popocatepetl volcanoes. Proceedings of the 2009 IEEE International Geoscience and Remote
678 Sensing Symposium, 2, II-1012.

679 Cortés, G., Benitez, M. C., García, L., Álvarez, I., & Ibanez, J. M. (2015), A comparative study of
680 dimensionality reduction algorithms applied to volcano-seismic signals. *IEEE Journal of Selected*
681 *Topics in Applied Earth Observations and Remote Sensing, 9*(1), 253–263.
682 doi:10.1109/JSTARS.2015.2479300

683 Cortés, G., García, L., Álvarez, I., Benítez, C., de la Torre, Á., & Ibáñez, J. (2014), Parallel system
684 architecture (PSA): An efficient approach for automatic recognition of volcano-seismic events.
685 *Journal of Volcanology and Geothermal Research, 271*, 1–10.
686 doi:10.1016/j.jvolgeores.2013.07.004

687 Cortés, G., Carniel, R., Mendoza, M. Á., & Lesage, P. (2019). Standardization of noisy volcanoseismic
688 waveforms as a key step toward station-independent, robust automatic recognition. Seismological
689 Research Letters, 90(2A), 581-590. doi:10.1785/0220180334

690 Cortés, G., Carniel, R., Lesage, P., Mendoza, M. Á., & Della Lucia, I. (2021). Practical volcano-
691 independent recognition of seismic events: VULCAN. ears project. Frontiers in Earth Science, 8,
692 616676. doi.org/10.3389/feart.2020.616676.

693 Caudron, C., Chardot, L., Girona, T., Aoki, Y., & Fournier, N. (2020), Towards improved forecasting of
694 volcanic eruptions. *Frontiers in Earth Science, 8*, 45. doi:10.3389/feart.2020.00045

695 Caudron, C., Girona, T., Jolly, A., Christenson, B., Savage, M. K., Carniel, R., et al. (2021), A quest for
696 unrest in multiparameter observations at Whakaari/White Island volcano, New Zealand 2007–
697 2018. *Earth, Planets and Space, 73*(1), 1–21. doi:10.1186/s40623-021-01506-0

698 Davydova, V. O., Shcherbakov, V. D., Plechov, P. Y., & Koulakov, I. Y. (2022), Petrological evidence of
699 rapid evolution of the magma plumbing system of Bezymianny volcano in Kamchatka before the
700 December 20th, 2017 eruption. *Journal of Volcanology and Geothermal Research, 421*, 107422.
701 doi:10.1016/j.jvolgeores.2021.107422

702 Dempsey, D. E., Cronin, S. J., Mei, S., & Kempa-Liehr, A. W. (2020), Automatic precursor recognition
703 and real-time forecasting of sudden explosive volcanic eruptions at Whakaari, New Zealand.
704 *Nature Communications, 11*(1), 1–8. doi:10.1038/s41467-020-17375-2

705 Dempsey, D. E., Kempa-Liehr, A. W., Ardid, A., Li, A., Orenia, S., Singh, J., ... & Cronin, S. J. (2022).
706 Evaluation of short-term probabilistic eruption forecasting at Whakaari, New Zealand. Bulletin of
707 Volcanology, 84(10), 91.

DeRoin, N., & McNutt, S. R. (2012), Rockfalls at Augustine Volcano, Alaska: The influence of eruption precursors and seasonal factors on occurrence patterns 1997–2009. *Journal of Volcanology and Geothermal Research, 211*, 61–75. doi:10.1016/j.jvolgeores.2011.11.0

DeShon, H. R., Thurber, C. H., & Power, J. A. (2010), Earthquake waveform similarity and evolution at Augustine Volcano from 1993 to 2006. In Power, J. A., Coombs, M. L., and Freymueller, J. T., (Eds.), *The 2006 Eruption of Augustine Volcano, Alaska* (pp. 103–118). U.S. Geological Survey Professional Paper 1769. https://pubs.usgs.gov/pp/1769/chapters/p1769_chapter05.pdf

De Siena, L., Thomas, C., Waite, G. P., Moran, S. C., & Klemme, S. (2014), Attenuation and scattering tomography of the deep plumbing system of Mount St. Helens. *Journal of Geophysical Research: Solid Earth, 119*(11), 8223–8238. doi:10.1002/2014JB011372

Di Luccio, F., Persaud, P., Cucci, L., Esposito, A., Carniel, R., Cortés, G., ... & Ventura, G. (2021). The seismicity of dynamically active Lipari, Aeolian Islands (Italy) from one-month recording of the LIPARI array. Frontiers in Earth Science, 9, 592. doi: 10.3389/feart.2021.678581

Endo, E. T., & Murray, T. (1991), Real-time seismic amplitude measurement (RSAM): a volcano monitoring and prediction tool. *Bulletin of Volcanology, 53*(7), 533–545. doi:10.1007/BF00298154

Esmaili, S., Krishnan, S., & Raahemifar, K. (2004), Content based audio classification and retrieval using joint time-frequency analysis. Proceeedings of the 2004 IEEE International Conference on Acoustics, Speech, and Signal Processing, 5, V-665).

Farquharson, J. I., & Amelung, F. (2020), Extreme rainfall triggered the 2018 rift eruption at Kīlauea Volcano. *Nature, 580*(7804), 491–495. doi:10.1038/s41586-020-2172-5

Gabrielli, S., De Siena, L., Napolitano, F., & Del Pezzo, E. (2020), Understanding seismic path biases and magmatic activity at Mount St Helens volcano before its 2004 eruption. *Geophysical Journal International, 222*(1), 169–188. doi:10.1093/gji/ggaa154

Girina, O. A. (2013), Chronology of Bezymianny volcano activity, 1956–2010. *Journal of Volcanology and Geothermal Research, 263*, 22–41. doi:10.1016/j.jvolgeores.2013.05.002

Girona, T., Caudron, C., & Huber, C. (2019), Origin of shallow volcanic tremor: the dynamics of gas pockets trapped beneath thin permeable media. Journal of Geophysical Research: Solid Earth, 124(5), 4831-4861. doi:10.1029/2019JB017482

Girona, T., Realmuto, V., & Lundgren, P. (2021), Large-scale thermal unrest of volcanoes for years prior to eruption. *Nature Geoscience, 14*(4), 238–241. doi:10.1038/s41561-021-00705-4

739 Gutiérrez, L., Ibáñez, J., Cortés, G., Ramírez, J., Benítez, C., Tenorio, V., & Isaac, A. (2009), Volcano-
740 seismic signal detection and classification processing using hidden Markov models. Application
741 to San Cristóbal volcano, Nicaragua. Proceedings of the 2009 IEEE International Geoscience and
742 Remote Sensing Symposium, 4, IV-522).

743 Ibáñez, J. M., Benítez, C., Gutiérrez, L. A., Cortés, G., García-Yeguas, A., & Alguacil, G. (2009), The
744 classification of seismo-volcanic signals using Hidden Markov Models as applied to the
745 Stromboli and Etna volcanoes. *Journal of Volcanology and Geothermal Research, 187*(3–4),
746 218–226. doi:10.1016/j.jvolgeores.2009.09.002

747 Ibáñez, J. M., Pezzo, E. D., Almendros, J., La Rocca, M., Alguacil, G., Ortiz, R., & García, A. (2000),
748 Seismovolcanic signals at Deception Island volcano, Antarctica: Wave field analysis and source
749 modeling. *Journal of Geophysical Research: Solid Earth, 105*(B6), 13905–13931.

750 Iverson, R. M., Dzurisin, D., Gardner, C. A., Gerlach, T. M., LaHusen, R. G., Lisowski, M., et al. (2006),
751 Dynamics of seismogenic volcanic extrusion at Mount St Helens in 2004–05. *Nature, 444*(7118),
752 439–443. doi:10.1038/nature05322

753 Jolly, A., Caudron, C., Girona, T., Christenson, B., & Carniel, R. (2020), 'Silent'dome emplacement into
754 a wet volcano: observations from an effusive eruption at White Island (Whakaari), New Zealand
755 in late 2012. *Geosciences, 10*(4), 142. doi:10.3390/geosciences10040142

756 Kilburn, C. R. (2018), Forecasting volcanic eruptions: Beyond the failure forecast method. *Frontiers in*
757 *Earth Science, 133*. doi:10.3389/feart.2018.00133

758 Konstantinou, K. I., & Schlindwein, V. (2003). Nature, wavefield properties and source mechanism of
759 volcanic tremor: a review. Journal of volcanology and geothermal research, 119(1-4), 161-187.

760 Koulakov, I., Plechov, P., Mania, R., Walter, T. R., Smirnov, S. Z., Abkadyrov, I., et al. (2021), Anatomy
761 of the Bezymianny volcano merely before an explosive eruption on 20.12. 2017. *Scientific*
762 *Reports, 11*(1), 1–12. doi:10.1038/s41598-021-81498-9

763 Lehto, H. L., Roman, D. C., & Moran, S. C. (2010), Temporal changes in stress preceding the 2004–2008
764 eruption of Mount St. Helens, Washington. *Journal of Volcanology and Geothermal Research,*
765 *198*(1–2), 129–142. doi:10.1016/j.jvolgeores.2010.08.015

766 Malfante, M., Dalla Mura, M., Mars, J. I., Métaxian, J. P., Macedo, O., & Inza, A. (2018a), Automatic
767 classification of volcano seismic signatures. *Journal of Geophysical Research: Solid Earth,*
768 *123*(12), 10,645-10,658. doi:10.1029/2018JB015470

769 Malfante, M., Dalla Mura, M., Métaxian, J. P., Mars, J. I., Macedo, O., & Inza, A. (2018b), Machine
770 learning for volcano-seismic signals: Challenges and perspectives. *IEEE Signal Processing*
771 *Magazine*, *35*(2), 20–30. doi:10.1109/MSP.2017.2779166

772 Manga, M., Carn, S. A., Cashman, K. V., Clarke, A. B., Connor, C. B., Cooper, K. M., et al. (2017),
773 *Volcanic eruptions and their repose, unrest, precursors, and timing*. Washington, DC: the
774 National Academies Press. doi:10.17226/24650

775 Mania, R., Walter, T. R., Belousova, M., Belousov, A., & Senyukov, S. L. (2019), Deformations and
776 morphology changes associated with the 2016–2017 eruption sequence at Bezymianny Volcano,
777 Kamchatka. *Remote Sensing, 11*(11), 1278. doi:10.3390/rs11111278

778 Manley, G. F., Mather, T. A., Pyle, D. M., Clifton, D. A., Rodgers, M., Thompson, G., & Roman, D. C.
779 (2021), Machine Learning Approaches to Identifying Changes in Eruptive State Using Multi-
780 Parameter Datasets From the 2006 Eruption of Augustine Volcano, Alaska. *Journal of*
781 *Geophysical Research: Solid Earth, 126*(12), e2021JB022323. doi:10.1029/2021JB022323

782 Manley, G. F., Pyle, D. M., Mather, T. A., Rodgers, M., Clifton, D. A., Stokell, B. G., et al. (2020),
783 Understanding the timing of eruption end using a machine learning approach to classification of
784 seismic time series. *Journal of Volcanology and Geothermal Research, 401*, 106917.
785 doi:10.1016/j.jvolgeores.2020.1069

786 Martínez, V. L., Titos, M., Benítez, C., Badi, G., Casas, J. A., Craig, V. H. O., & Ibáñez, J. M. (2021),
787 Advanced signal recognition methods applied to seismo-volcanic events from Planchon Peteroa
788 Volcanic Complex: Deep Neural Network classifier. *Journal of South American Earth Sciences,*
789 *107*, 1–12, 103115. doi:10.1016/j.jsames.2020.103115

790 Massa, B., D'Auria, L., Cristiano, E., & De Matteo, A. (2016), Determining the stress field in active
791 volcanoes using focal mechanisms. *Frontiers in Earth Science, 4*, 103.
792 doi:10.3389/feart.2016.00103

793 McKee, K., Smith, C. M., Reath, K., Snee, E., Maher, S., Matoza, R. S., et al. (2021a), Evaluating the
794 state-of-the-art in remote volcanic eruption characterization Part I: Raikoke volcano, Kuril
795 Islands. *Journal of Volcanology and Geothermal Research, 419*, 107354.
796 doi:10.1016/j.jvolgeores.2021.107354

797 McKee, K., Smith, C. M., Reath, K., Snee, E., Maher, S., Matoza, R. S., et al. (2021b), Evaluating the
798 state-of-the-art in remote volcanic eruption characterization Part II: Ulawun volcano, Papua New

Guinea. *Journal of Volcanology and Geothermal Research, 420*, 107381. doi:10.1016/j.jvolgeores.2021.107381

McNutt, S. R., & Roman, D. C. (2015), Volcanic seismicity. In H. Sigurdsson (Ed.). *The Encyclopedia of Volcanoes* (2nd edition, pp. 1011–1034). Elsevier Inc. doi:10.1016/b978-0-12-385938-9.00059-6

Neal, C. A., Brantley, S. R., Antolik, L., Babb, J. L., Burgess, M., Calles, K., Cappos, M., Chang, J. C., Conway, S., Desmither, L., Dotray, P., Elias, T., Fukunaga, P., Fuke, S., Johanson, I. A., Kamibayashi, K., Kauahikaua, J., Lee, R. L., Pekalib, S., … Damby, D. (2019), The 2018 rift eruption and summit collapse of Kīlauea volcano. *Science, 363*(6425), 367–374. doi:10.1126/science.aav7046

Ortiz, R., Moreno, H., Garcıa, A., Fuentealba, G., Astiz, M., Peña, P., et al. (2003), Villarrica volcano (Chile): characteristics of the volcanic tremor and forecasting of small explosions by means of a material failure method. *Journal of Volcanology and Geothermal Research, 128*(1–3), 247–259. doi:10.1016/S0377-0273(03)00258-0

Patrick, M. R., Houghton, B. F., Anderson, K. R., Poland, M. P., Montgomery-Brown, E., Johanson, I., et al. (2020), The cascading origin of the 2018 Kīlauea eruption and implications for future forecasting. *Nature Communications, 11*(1), 1–13. doi:10.1038/s41467-020-19190-1

Posadas, A., Morales, J., Ibañez, J. M., & Posadas-Garzon, A. (2021), Shaking earth: Non-linear seismic processes and the second law of thermodynamics: A case study from Canterbury (New Zealand) earthquakes. *Chaos, Solitons & Fractals, 151*, 111243. doi:10.1016/j.chaos.2021.111243

Power, J. A., Coombs, M. L., & Freymueller, J. T. (Eds.). (2010). p., 1 plate, scale 1:20,000, and data files. In Power, J. A., Coombs, M. L., and Freymueller, J. T., (Eds.), *The 2006 Eruption of Augustine Volcano, Alaska*, U.S. Geological Survey Professional Paper 1769.

Power, J. A., Haney, M. M., Botnick, S. M., Dixon, J. P., Fee, D., Kaufman, A. M., et al. (2020), Goals and development of the Alaska Volcano Observatory seismic network and application to forecasting and detecting volcanic eruptions. *Seismological Research Letters, 91*(2A), 647–659. doi:10.1785/0220190216

Power, J. A., Stihler, S. D., Chouet, B. A., Haney, M. M., & Ketner, D. M. (2013), Seismic observations of Redoubt Volcano, Alaska—1989–2010 and a conceptual model of the Redoubt magmatic system. *Journal of Volcanology and Geothermal Research, 259*, 31–44. doi:10.1016/j.jvolgeores.2012.09.014

829 Presti, D. L., Riggi, F., Ferlito, C., Bonanno, D. L., Bonanno, G., Gallo, G., et al. (2020), Muographic
830 monitoring of the volcano-tectonic evolution of Mount Etna. *Scientific Reports, 10*(1), 1–11.
831 doi:10.1038/s41598-020-68435-y

832 Pyle, D. M. (2015), Sizes of volcanic eruptions. In H. Sigurdsson (Ed.). *The Encyclopedia of Volcanoes*
833 (2nd edition, pp. 257–264). Elsevier Inc. (pp. 257–264). Academic Press. doi:10.1016/B978-0-12-
834 385938-9.00013-4

835 Ren, C. X., Peltier, A., Ferrazzini, V., Rouet-Leduc, B., Johnson, P. A., & Brenguier, F. (2020), Machine
836 learning reveals the seismic signature of eruptive behavior at piton de la fournaise volcano.
837 *Geophysical Research Letters, 47*(3), e2019GL085523. doi:10.1029/2019GL085523

838 Roman, D. C., Soldati, A., Dingwell, D. B., Houghton, B. F., Shiro, B. R. (2021), Earthquakes indicated
839 magma viscosity during Kīlauea's 2018 eruption. *Nature, 592*(7853), 237–241.
840 doi:10.1038/s41586-021-03400-x

841 Saccorotti, G., & Lokmer, I. (2021), A review of seismic methods for monitoring and understanding
842 active volcanoes. In P. Papale (Ed.). *Forecasting and Planning for Volcanic Hazards, Risks, and*
843 *Disasters* (vol. 2, pp. 25–73). Elsevier Inc. doi:10.1016/b978-0-12-818082-2.00002-0

844 Sherrod, D. R., Scott, W. E., & Stauffer, P. H. (Eds.). (2008). A volcano rekindled: the renewed eruption
845 of Mount St. Helens, 2004–2006. U.S. Geological Survey Professional Paper 1750.

846 Spampinato, S., Langer, H., Messina, A., & Falsaperla, S. (2019), Short-term detection of volcanic unrest
847 at Mt. Etna by means of a multi-station warning system. *Scientific Reports, 9*(1), 1–10.
848 doi:10.1038/s41598-019-42930-3

849 Sparks, R. S. J., Biggs, J., & Neuberg, J. W. (2012), Monitoring volcanoes. *Science, 335*(6074), 1310–
850 1311. doi:10.1126/science.1219485

851 Thelen, W. A., Matoza, R. S., & Hotovec-Ellis, A. J. (2022), Trends in volcano seismology: 2010 to 2020
852 and beyond. *Bulletin of Volcanology, 84*, 26. doi:10.1007/s00445-022-01530-2

853 Thelen, W., West, M., & Senyukov, S. (2010), Seismic characterization of the fall 2007 eruptive sequence
854 at Bezymianny Volcano, Russia. *Journal of Volcanology and Geothermal Research, 194*(4), 201–
855 213. doi:10.1016/j.jvolgeores.2010.05.010

856 Titos, M., Bueno, A., Garcia, L., & Benitez, C. (2018a), A deep neural networks approach to automatic
857 recognition systems for volcano-seismic events. *IEEE Journal of Selected Topics in Applied*
858 *Earth Observations and Remote Sensing, 11*(5), 1533–1544. doi:10.1109/JSTARS.2018.2803198

Titos, M., Bueno, A., García, L., Benítez, M. C., & Ibañez, J. (2018b), Detection and classification of continuous volcano-seismic signals with recurrent neural networks. *IEEE Transactions on Geoscience and Remote Sensing, 57*(4), 1936–1948. doi:10.1109/TGRS.2018.2870202

Titos, M., Bueno, A., García, L., Benítez, C., & Segura, J. C. (2019), Classification of isolated volcano-seismic events based on inductive transfer learning. *IEEE Geoscience and Remote Sensing Letters, 17*(5), 869–873. doi:10.1109/LGRS.2019.2931063

Titos, M., García, L., Kowsari, M., & Benítez, C. (2022), Toward Knowledge Extraction in Classification of Volcano-Seismic Events: Visualizing Hidden States in Recurrent Neural Networks. *IEEE Journal of Selected Topics in Applied Earth Observations and Remote Sensing, 15*, 2311–2325. doi:10.1109/JSTARS.2022.3155967

Trujillo-Castrillón, N., Valdés-González, C. M., Arámbula-Mendoza, R., & Santacoloma-Salguero, C. C. (2018), Initial processing of volcanic seismic signals using Hidden Markov Models: Nevado del Huila, Colombia. *Journal of Volcanology and Geothermal Research, 364*, 107–120. doi:10.1016/j.jvolgeores.2018.09.008

van Ruitenbeek, F. J., Goseling, J., Bakker, W. H., & Hein, K. A. (2020), Shannon entropy as an indicator for sorting processes in hydrothermal systems. *Entropy, 22*(6), 656. doi:10.3390/e22060656

Whitehead, M. G., & Bebbington, M. S. (2021), Method selection in short-term eruption forecasting. *Journal of Volcanology and Geothermal Research, 419*, 107386. doi:10.1016/j.jvolgeores.2021.107386

Zhan, Y., Le Mével, H., Roman, D. C., Girona, T., & Gregg, P. M. (2022), Modeling deformation, seismicity, and thermal anomalies driven by degassing during the 2005-2006 pre-eruptive unrest of Augustine Volcano, Alaska. *Earth and Planetary Science Letters, 585*, 117524. doi:10.1016/j.epsl.2022.11752

Zuccarello, L., De Angelis, S., Minio, V., Saccorotti, G., Bean, C. J., Paratore, M., & Ibanez, J. M. (2022). Volcanic Tremor Tracks Changes in Multi-Vent Activity at Mt. Etna, Italy: Evidence From Analyses of Seismic Array Data. Geophysical Research Letters, 49(22), e2022GL100056.

889 TABLES

890

891 **Table 1.** Volcanic Data and Seismic Stations

VOLCANO (LOCATION)	PERIOD	SEISMIC STATION	DESCRIPTION AND ACTIVITY	MONITORING	REFERENCES
Mt.Etna (Sicily, Italy)	November 2013 11th,17th, 23rd, 28th	EBEM	Basaltic Stratovolcano. Volcanic tremor. Strombolian activity and Lava Fountain	INGV-OE (Instituto Nazionale di Geofisica e Vulcanologia – Osservatorio Etneo)	Aloisi et al., 2020; Barreca et al., 2018, 2020; Presti et al., 2020; Bonaccorso et al., 2014 Spampinato et al., 2019 Zuccarello et al., 2022
Bezymianny (Kamchatka, Russia)	December 20th, 2017 September 25th October 14th, November 5th, 2007	BZ01 (Fig. 2: blue) BELO (Fig. 2: green)	Andesitic volcano. VT activity. Dome growth. Very energetic explosions	Temporary Field Experiment (2017) KGBS (Kamchatkan Branch of Geophysical Survey)	Mania et al., 2019 Koulakov et al., 2021 Davydova et al., 2022 Girina, 2013 Thelen et al., 2010 Bueno et al, 2019
Mount St. Helens (Washington, USA)	October 1st , 2004	SHW	Andesitic-Dacitic Stratovolcano. VT and tremor. Phreatic Eruption	Pacific Northwest Seismic Network University of Washington	Iverson et al., 2006 De Siena et al., 2014 Sherrod et al., 2008 Berlo et al., 2004 Gabrielli et al., 2020 Anderson & Segall, 2013 Lehto et al., 2010
Augustine (Alaska, USA)	January 11th, 2006	AUH	Andesitic-Dacitic Stratovolcano VT activity. Vulcanian activity	AVO (Alaska Volcano Observatory)	DeRoin & McNutt, 2012 DeShon et al., 2010 Buurman & West, 2006 Bailey et al., (2006) Coombs et al., 2010 Manley et al., 2021 Power et al., 2010 Zhan et al., 2022
Kilauea (Hawaii, USA)	May 3rd, 2018	JOKA	Basaltic Shield Volcano Summit Collapse and fissure eruptions	HVO (Hawaiian Volcano Observatory)	Patrick et al., 2020 Neal et al., 2019 Roman et al., 2021

892 **FIGURE CAPTIONS.**

893 **Figure 1.** Schematic workflow illustrating the methodology used to transform the seismic data from the amplitude-
894 time space of seismograms to the temporal matrix space of features.

895 **Figure 2.** Study region locations and maps of the seismic networks for each of the five volcanoes: Mount St.
896 Helens, Bezymianny, Augustine, Kilauea and Mt. Etna. Red triangles denote the main eruptive center, squares
897 represent the used seismic stations and blue square are the seismic stations used to plot the figures of this work. In
898 the map of the Bezymianny volcano we denoted in black triangle and with a letter K the position of the volcano
899 Kliuchevskoy and added the letter B to the main eruptive center of Bezymianny volcano. In Bezymianny map blue
900 square represents the station BZ01 and the green square is the station BELO.

901 **Figure 3**. Temporal variation of Shannon Entropy at station BZ01 of Bezymianny from August 2017 to July 2018.
902 The biggest decay occurred in the instant of the largest volcanic explosion of December, 20th 2017. Additional low
903 Shannon entropy values were observed. Data from the KBGS (Kamchatka Branch Geophysical Survey) institution
904 reported two important explosions at the neighboring Kliuchevskoy volcano (August 2017 and May 2018) marked
905 as a red shadow area. There is a minimum of short duration located on September 2017 associated with a local
906 earthquake of magnitude Mw 4.3 as reported in IRIS institution. The decrease observed in March 2018 is associated
907 to an intense volcanic tremor recorded in the volcanic area triggered by another local earthquake of Mw 4.5
908 (reported in IRIS). In April 2018 an intense volcano-tectonic earthquake swarm was recorded, associated with a set
909 of three minimum values of the Shannon Entropy.

910 **Figure 4.** (Up)Temporal evolution of the Shannon entropy before and after eruptive episode of Bezymianny,
911 December 2017 marked with a vertical red line. Green region indicates a stable decay bigger than the 70%. Decay at
912 the moment of the eruption: 98.3%. (Down) Temporal evolution of the STA/LTA ratio making in red values bigger
913 than 70%.

914 **Figure 5.** Temporal evolution of the Shannon entropy before and after three explosive episodes of Bezymianny in
915 2007, all of them marked with vertical red lines. Green region indicates a decay bigger than the 70%. Decay at the
916 moment of the eruption: 99.5%, 99.5% and 100%.

917 **Figure 6.** Temporal evolution of the Shannon entropy before and after four lava fountain paroxysms of Mt. Etna
918 during November 2013 all of them marked with vertical red lines. Green region indicates a decay bigger than the
919 70%. Decay at the moment of the eruption: 98.4%, 98.9%, 97.4% and 95.1%.

920 **Figure** 7. a) Temporal evolution of the Shannon entropy before and after the October 1st, 2004, eruptive episode of
921 Mount St. Helens marked with the vertical red line. Blank spaces in the graph represent data gaps; the vertical red
922 line denote the time of the eruption. b) Temporal evolution of the Shannon entropy before and after the January
923 11th, 2006, eruption of Augustine. The two main explosions are marked with vertical red lines. c) Temporal
924 evolution of energy (blue line) and Shannon entropy (orange line) at Kilauea from April 29 to May 7, 2018. The
925 solid black line marks the caldera collapse and the dashed line marks a local Mw 6.9 earthquake. The solid red line

926 denotes the start of the eruptive episode. Green region indicates a decay bigger than the 70%. Decay at the moment
927 of the eruption in Mount St. Helens and Augustine: 100% and 96.8%. Kilauea: induced by summit collapse (99.1%),
928 first fissure (80.7%) and earthquake (98.0%).

929 **Figure 8.** Cumulative number of volcano tectonic (VT) earthquakes (orange line) and the temporal evolution of
930 kurtosis (blue line) at station BZ01 of Bezymianny prior to the explosion of December 20st, 2017 marked with the
931 vertical red line. Green region indicates a decay of the Shannon Entropy larger than the 70%.

932 **Figure 9.** (Upper figure) Comparison between the temporal evolution of the logarithm of the energy (orange line)
933 and the temporal evolution of Frequency Index (blue line) at station EBEM of Mt. Etna prior to the lava fountain of
934 November 23rd, 2013, marked with the vertical red line. Green region indicates decay of the Shannon Entropy
935 bigger than the 70% of the average value until the starting of the eruption. (Lower figure) seismogram and
936 spectrogram of the volcanic tremor associated to the lava fountain eruption.

937 **Figure 10.** Temporal evolution of energy, kurtosis, and frequency index prior to the eruption of Mount St. Helens,
938 October 2004, marked with the vertical red line. Green region indicates a decay bigger than the 70%.

Figure1.

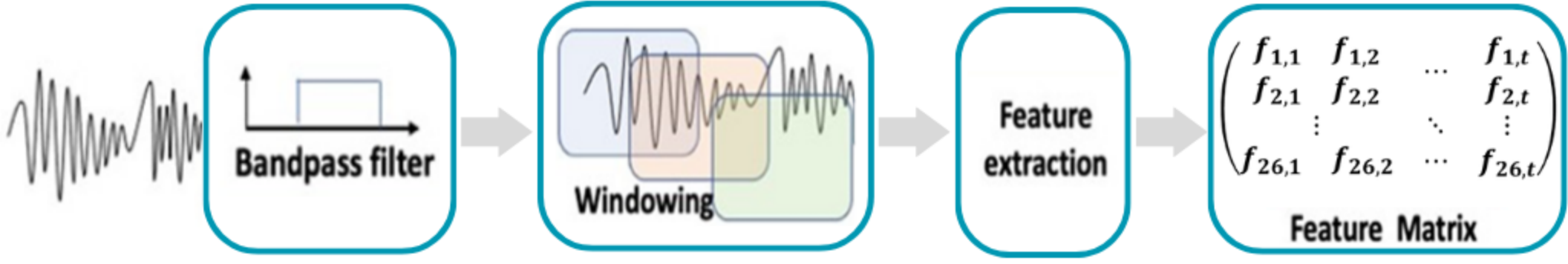
Bandpass filter
Windowing
Feature extraction
$\begin{pmatrix} f_{1,1} & f_{1,2} & \cdots & f_{1,t} \\ f_{2,1} & f_{2,2} & & f_{2,t} \\ \vdots & & \ddots & \vdots \\ f_{26,1} & f_{26,2} & \cdots & f_{26,t} \end{pmatrix}$
Feature Matrix

Figure2.

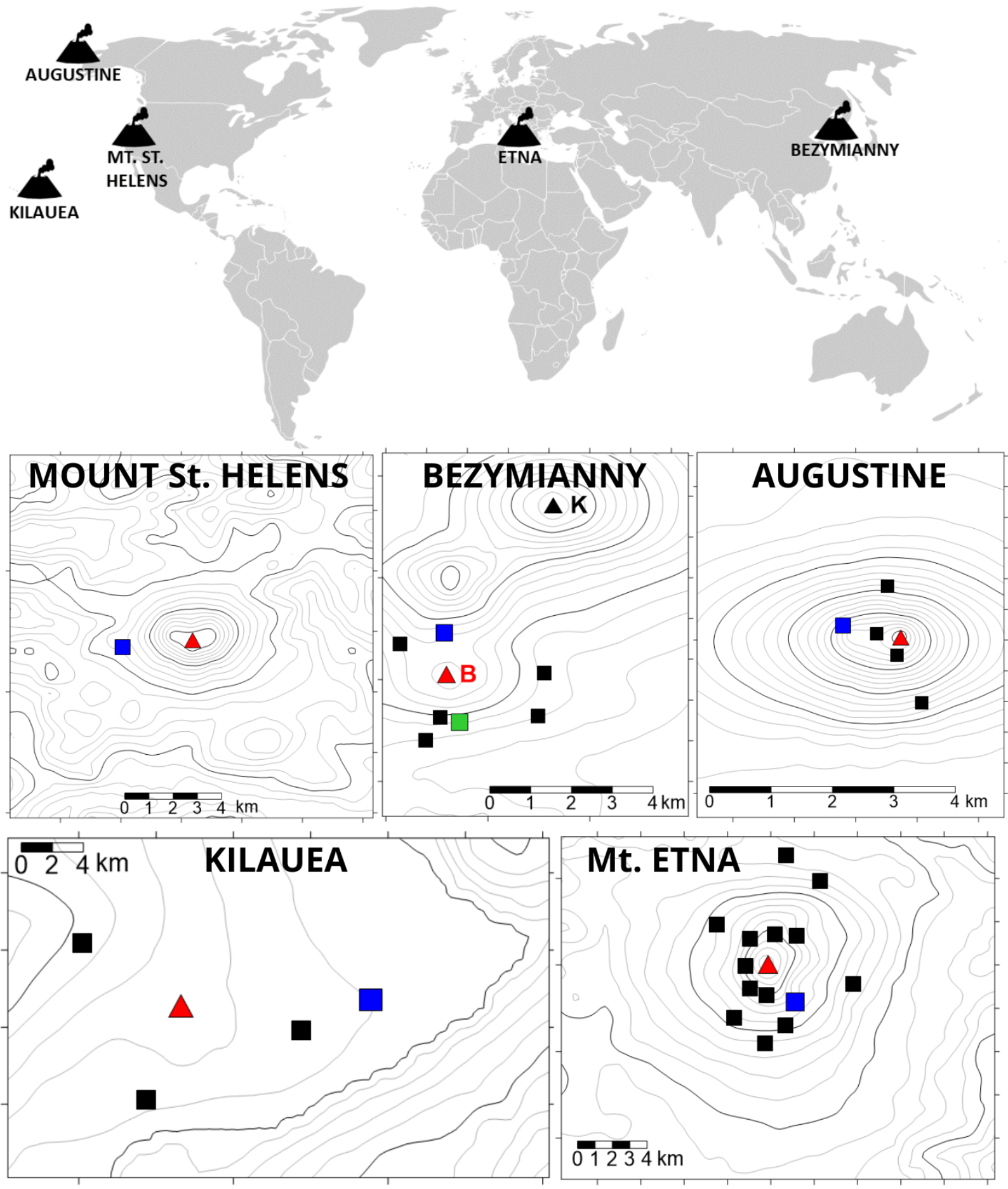
AUGUSTINE
MT. ST. HELENS
KILAUEA
ETNA
BEZYMIANNY
MOUNT St. HELENS
0 1 2 3 4 km
BEZYMIANNY
K
B
0 1 2 3 4 km
AUGUSTINE
0 1 2 3 4 km
0 2 4 km
KILAUEA
Mt. ETNA
0 1 2 3 4 km

Figure3.

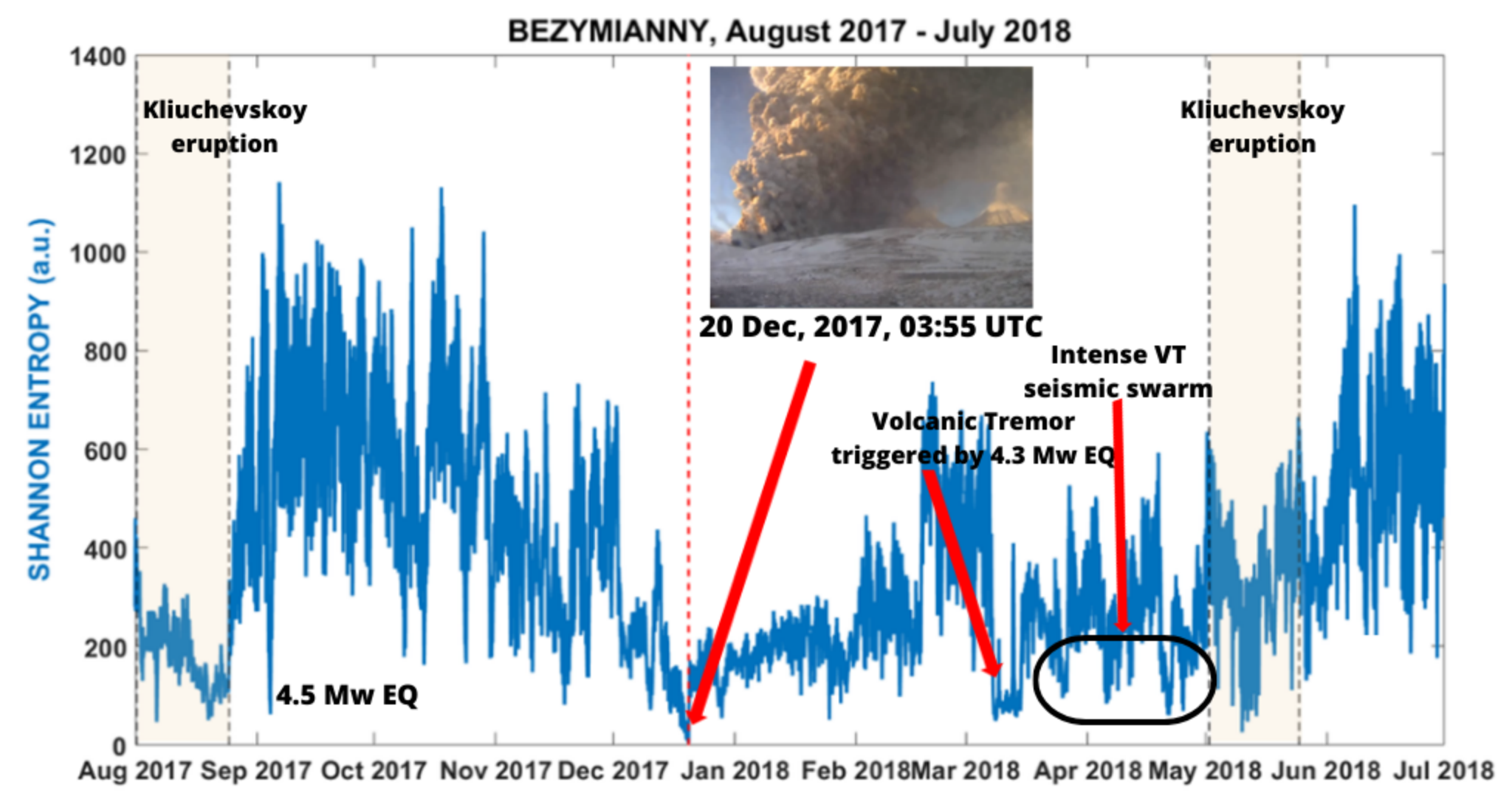
BEZYMIANNY, August 2017 - July 2018
SHANNON ENTROPY (a.u.)
1400
1200
1000
800
600
400
200
0
Kliuchevskoy eruption
Kliuchevskoy eruption
20 Dec, 2017, 03:55 UTC
Intense VT seismic swarm
Volcanic Tremor triggered by 4.3 Mw EQ
4.5 Mw EQ
Aug 2017
Sep 2017
Oct 2017
Nov 2017
Dec 2017
Jan 2018
Feb 2018
Mar 2018
Apr 2018
May 2018
Jun 2018
Jul 2018

Figure4.

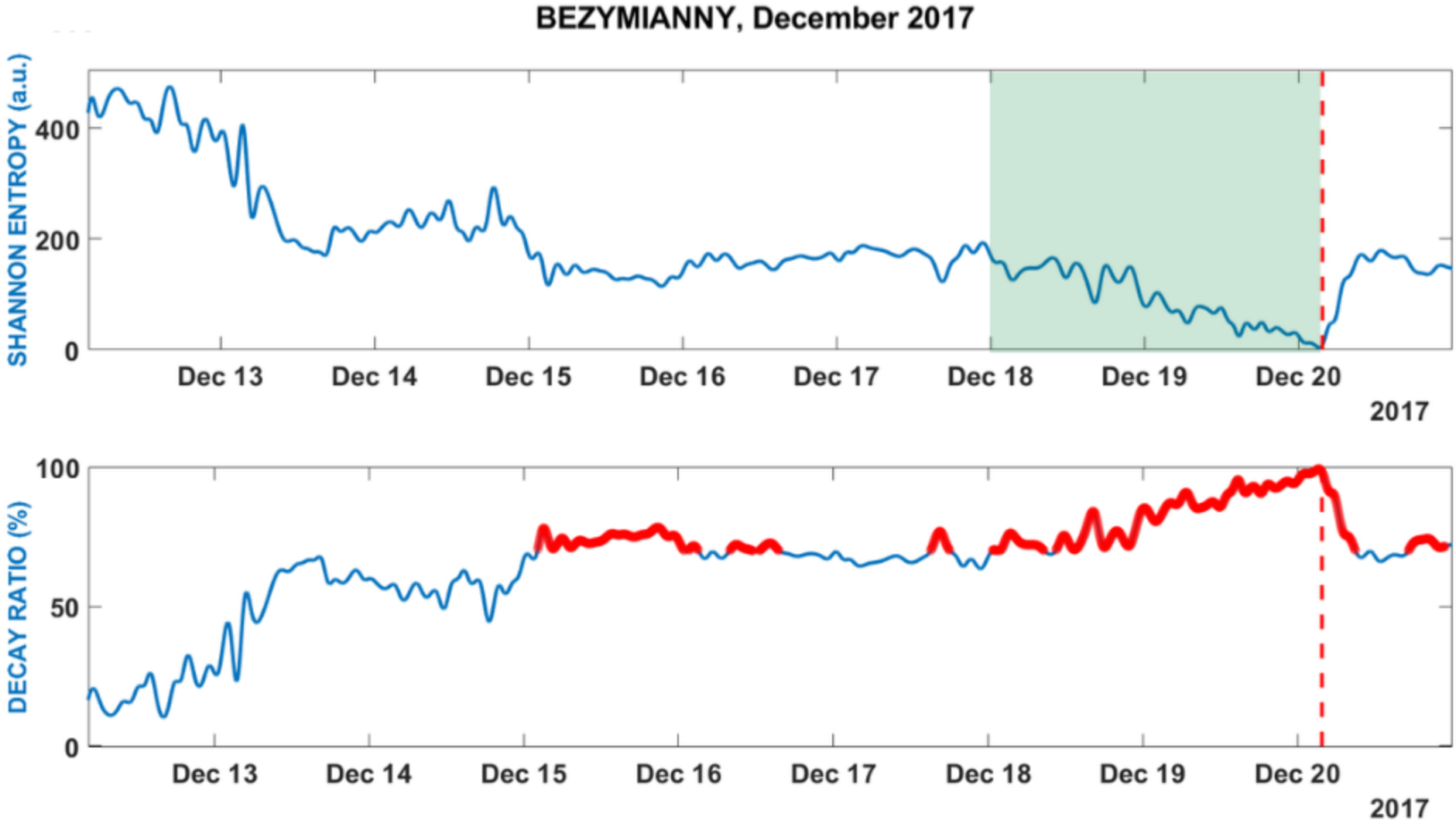
BEZYMIANNY, December 2017
SHANNON ENTROPY (a.u.)
400
200
0
Dec 13
Dec 14
Dec 15
Dec 16
Dec 17
Dec 18
Dec 19
Dec 20
2017
DECAY RATIO (%)
100
50
0
Dec 13
Dec 14
Dec 15
Dec 16
Dec 17
Dec 18
Dec 19
Dec 20
2017

Figure5.

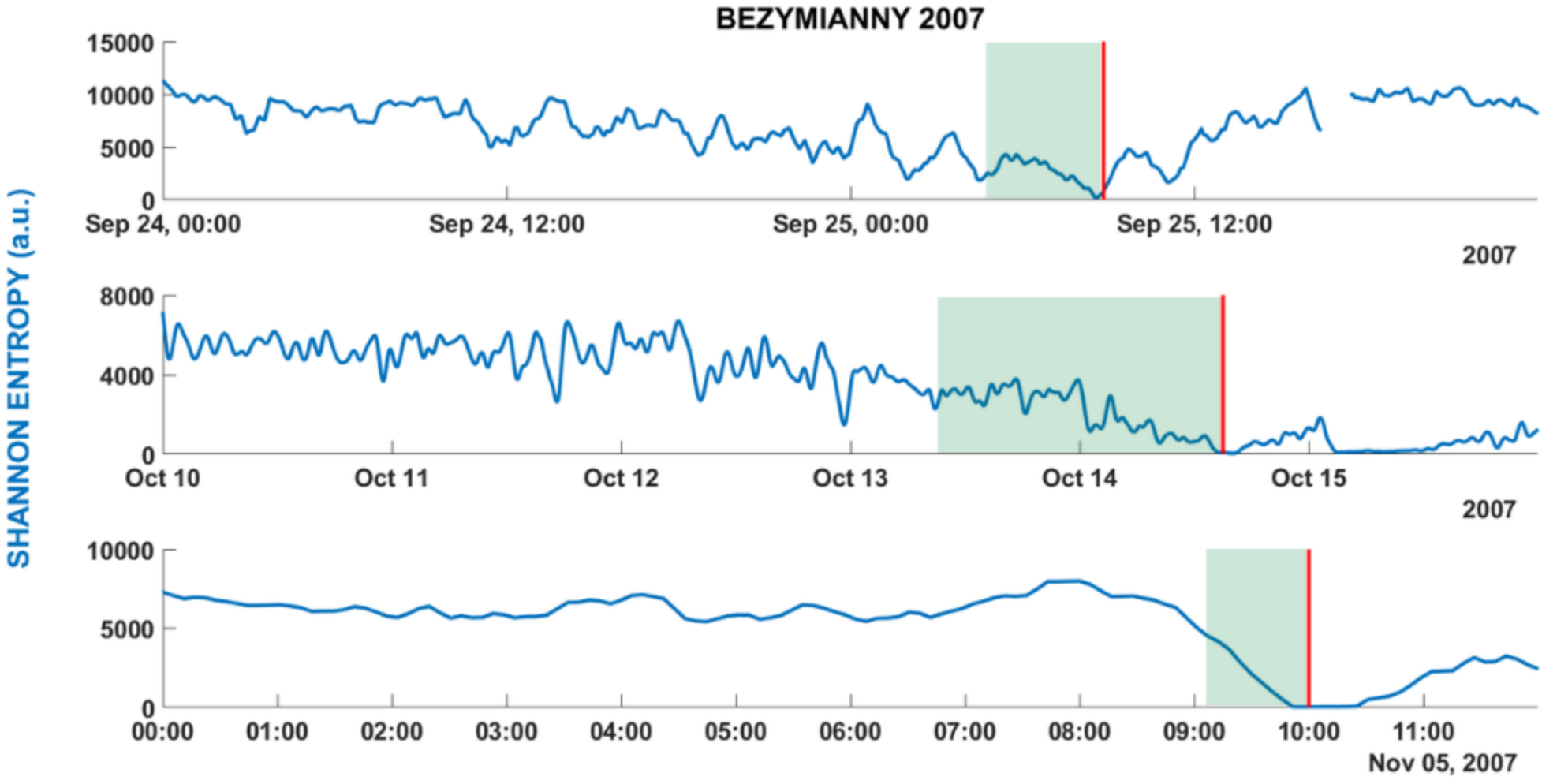
BEZYMIANNY 2007
SHANNON ENTROPY (a.u.)
15000
10000
5000
0
Sep 24, 00:00
Sep 24, 12:00
Sep 25, 00:00
Sep 25, 12:00
2007
8000
4000
0
Oct 10
Oct 11
Oct 12
Oct 13
Oct 14
Oct 15
2007
10000
5000
0
00:00
01:00
02:00
03:00
04:00
05:00
06:00
07:00
08:00
09:00
10:00
11:00
Nov 05, 2007

Figure6.

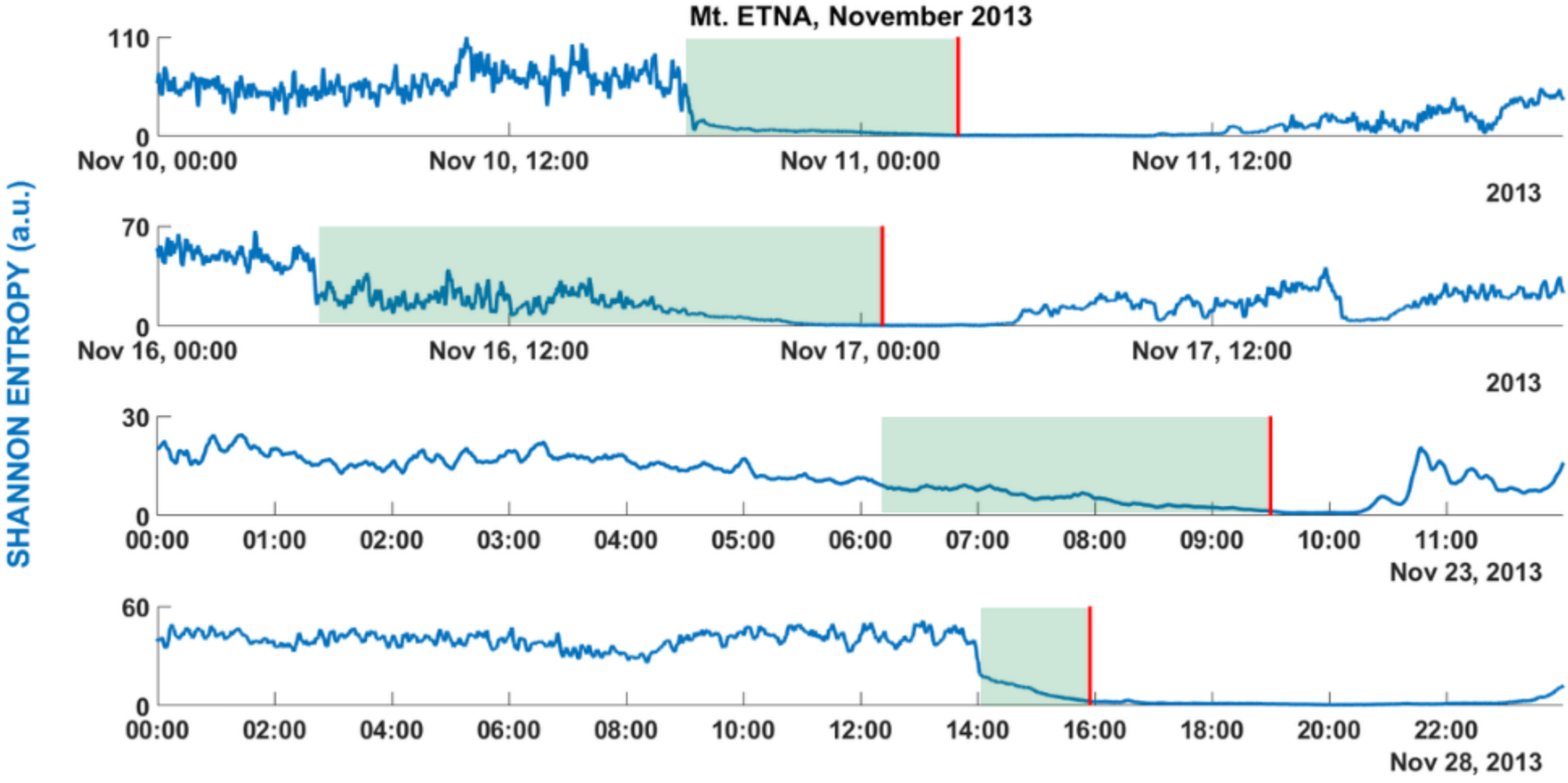
Mt. ETNA, November 2013
SHANNON ENTROPY (a.u.)
110
0
Nov 10, 00:00
Nov 10, 12:00
Nov 11, 00:00
Nov 11, 12:00
2013
70
0
Nov 16, 00:00
Nov 16, 12:00
Nov 17, 00:00
Nov 17, 12:00
2013
30
0
00:00
01:00
02:00
03:00
04:00
05:00
06:00
07:00
08:00
09:00
10:00
11:00
Nov 23, 2013
60
0
00:00
02:00
04:00
06:00
08:00
10:00
12:00
14:00
16:00
18:00
20:00
22:00
Nov 28, 2013

Figure7.

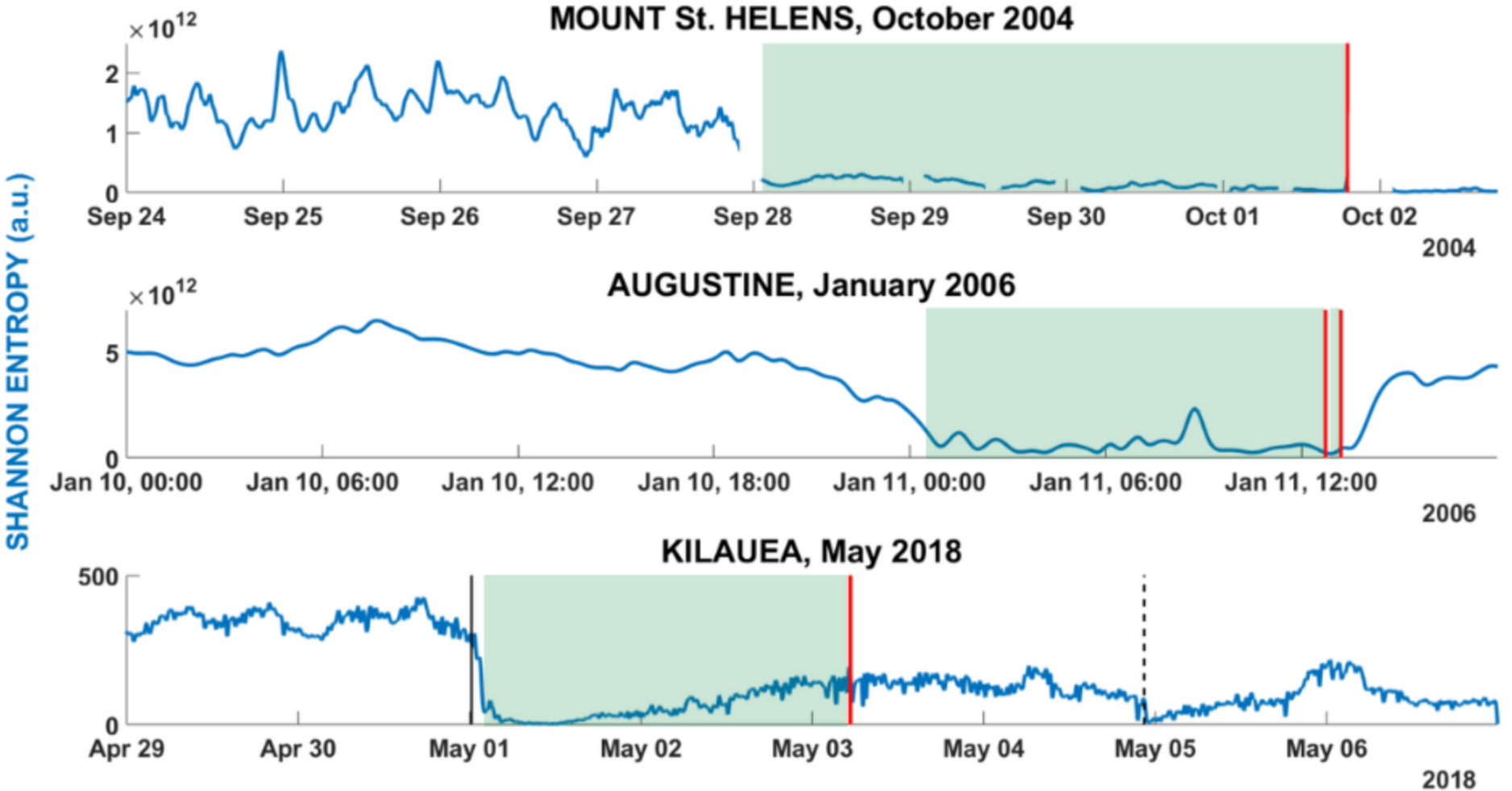
MOUNT St. HELENS, October 2004
×10^12
2
1
0
Sep 24
Sep 25
Sep 26
Sep 27
Sep 28
Sep 29
Sep 30
Oct 01
Oct 02
2004
AUGUSTINE, January 2006
×10^12
5
0
Jan 10, 00:00
Jan 10, 06:00
Jan 10, 12:00
Jan 10, 18:00
Jan 11, 00:00
Jan 11, 06:00
Jan 11, 12:00
2006
KILAUEA, May 2018
500
0
Apr 29
Apr 30
May 01
May 02
May 03
May 04
May 05
May 06
2018
SHANNON ENTROPY (a.u.)

Figure8.

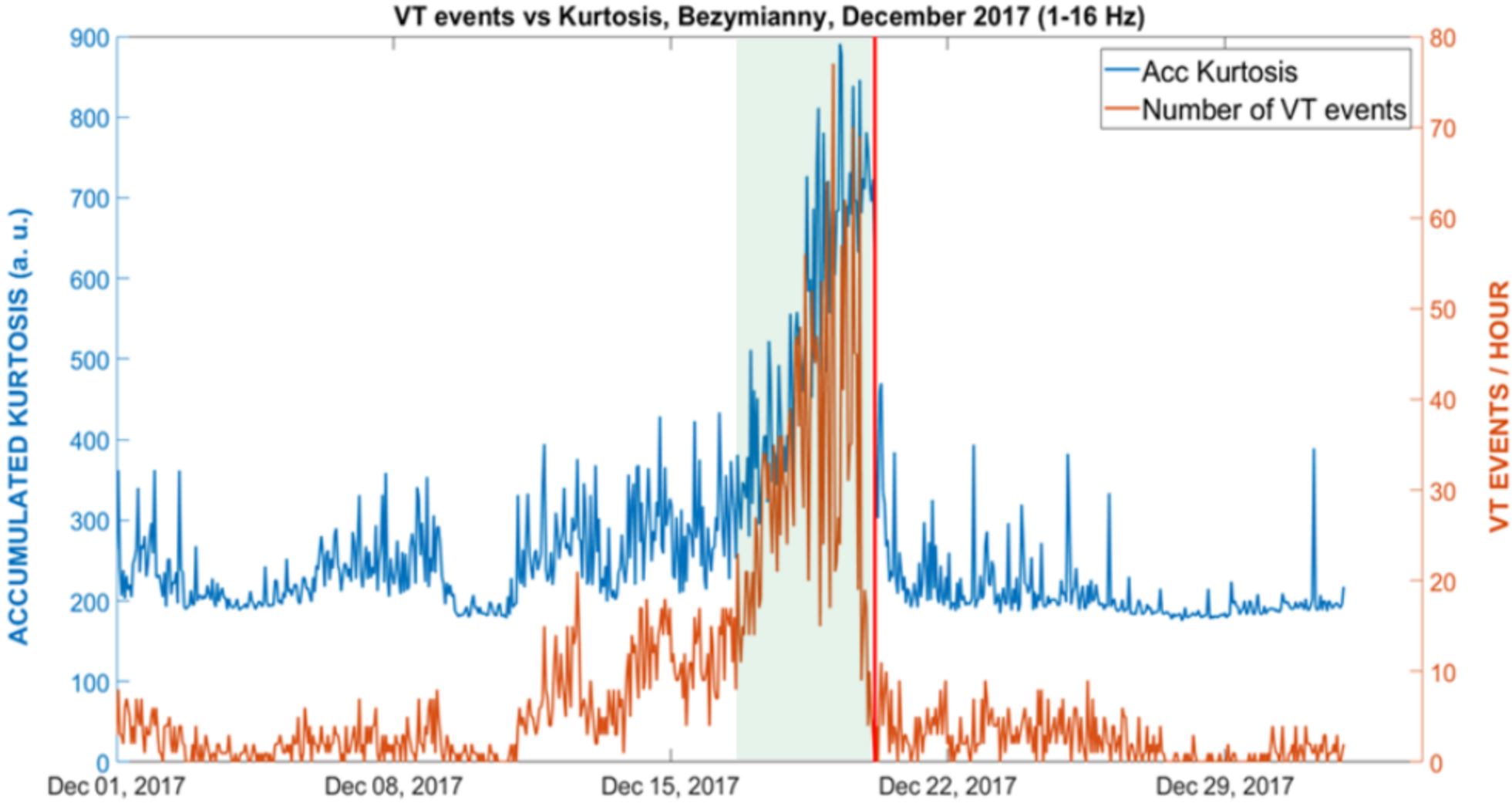
VT events vs Kurtosis, Bezymianny, December 2017 (1-16 Hz)
Acc Kurtosis
Number of VT events
ACCUMULATED KURTOSIS (a. u.)
VT EVENTS / HOUR
0
100
200
300
400
500
600
700
800
900
0
10
20
30
40
50
60
70
80
Dec 01, 2017
Dec 08, 2017
Dec 15, 2017
Dec 22, 2017
Dec 29, 2017

Figure9.

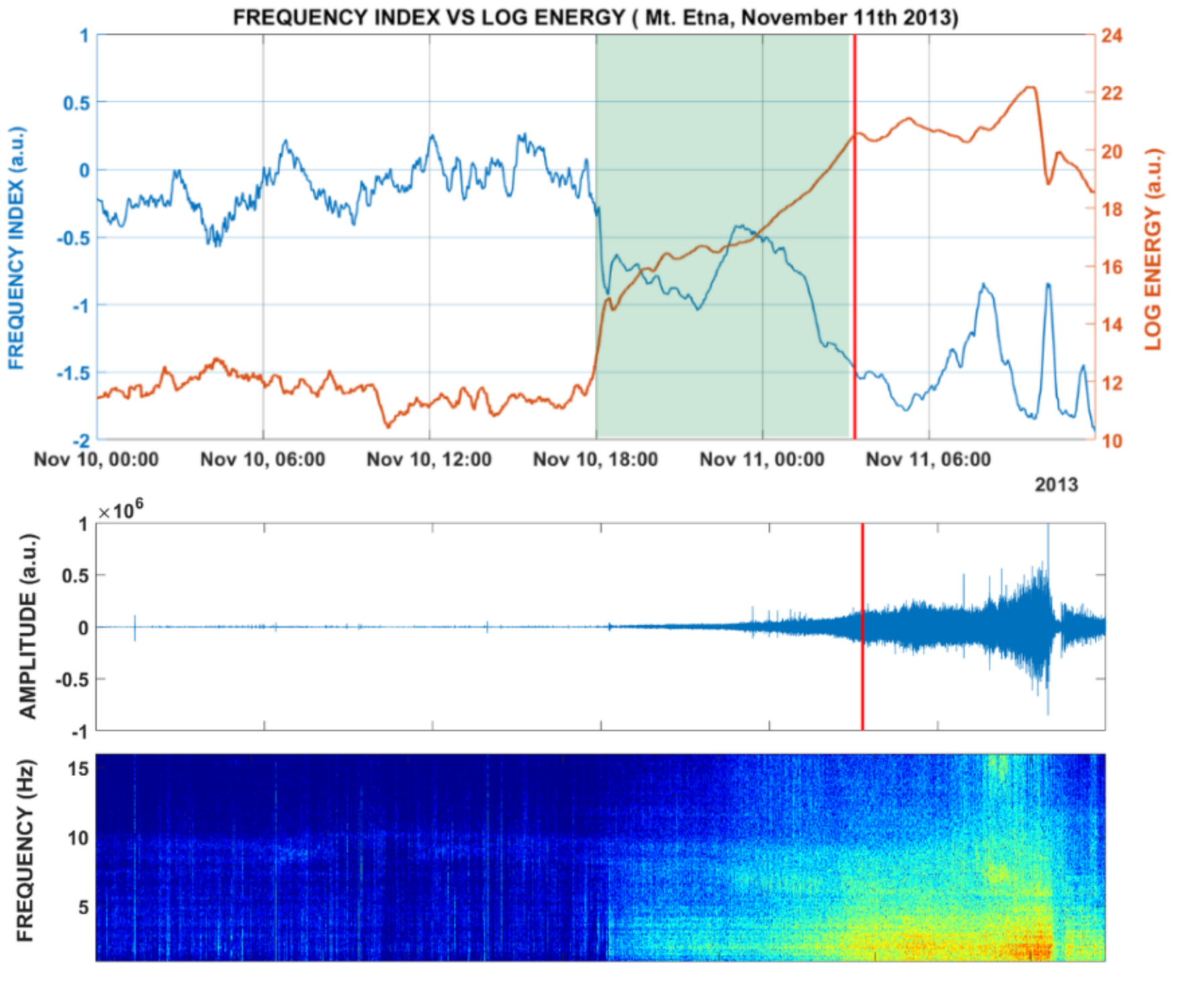
FREQUENCY INDEX VS LOG ENERGY (Mt. Etna, November 11th 2013)
FREQUENCY INDEX (a.u.)
LOG ENERGY (a.u.)
1
0.5
0
-0.5
-1
-1.5
-2
24
22
20
18
16
14
12
10
Nov 10, 00:00
Nov 10, 06:00
Nov 10, 12:00
Nov 10, 18:00
Nov 11, 00:00
Nov 11, 06:00
2013
×10^6
AMPLITUDE (a.u.)
1
0.5
0
-0.5
-1
FREQUENCY (Hz)
15
10
5

Figure10.

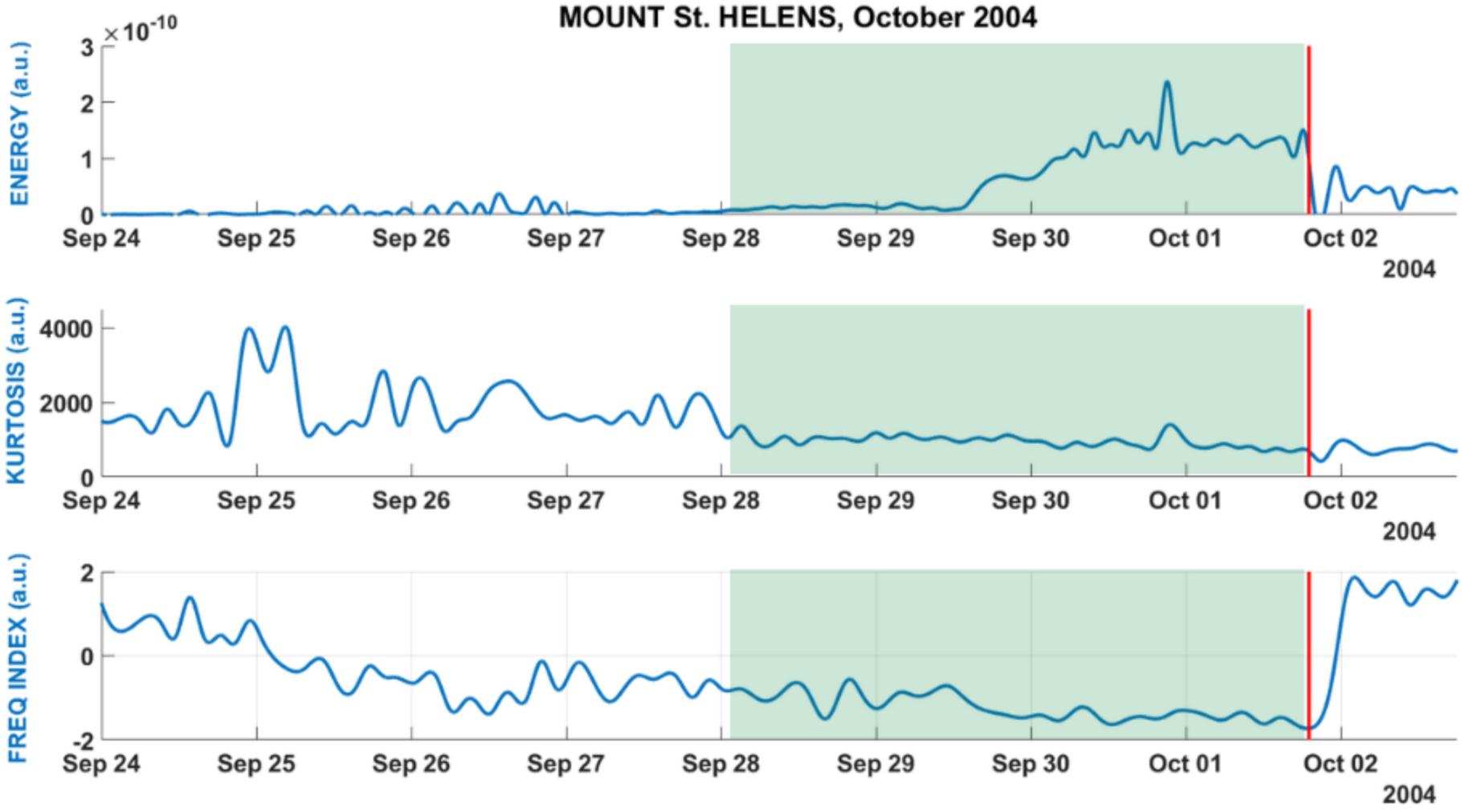
MOUNT St. HELENS, October 2004
ENERGY (a.u.)
×10-10
3
2
1
0
KURTOSIS (a.u.)
4000
2000
0
FREQ INDEX (a.u.)
2
0
-2
Sep 24
Sep 25
Sep 26
Sep 27
Sep 28
Sep 29
Sep 30
Oct 01
Oct 02
2004